Received: Added at production | Revised: Added at production | Accepted: Added at production

DOI: xxx/xxxx

ARTICLE TYPE

# Active fault detection based on set-membership approach for uncertain discrete-time systems

Jing Wang[1] | Yuru Shi[1] | Meng Zhou*[1] | Ye Wang[2] | Vicenç Puig[3]

[1]College of Information Science and Technology, Beijing University of Chemical Technology, Beijing, China
[2]College of Automation, Harbin Engineering University, Harbin, China
[3]Advanced Control Systems Research Group at Institutde Robòtical, CSIC-UPC, Universitat Politècnica de Catalunya-BarcelonaTech, Barcelone, Spain

**Correspondence**
*Meng Zhou, College of Information Science and Technology, Beijing University of Chemical Technology, Beijing 100029, China . Email: zhoumeng@mail.buct.edu.cn

**Summary**

Active fault detection facilitates determination of the fault characteristics by injecting proper auxiliary input signals into the system. This paper proposes an observer-based on-line active fault detection method for discrete-time systems with bounded uncertainties. First, the output including disturbances, measurement noise and interval uncertainties at each sample time is enclosed in a zonotope. In order to reduce the conservativeness in the fault detection process, a zonotopic observer is designed to estimate the system states allowing to generate the output zonotopes. Then, a proper auxiliary input signal is designed to separate the output zonotopes of the faulty model from the healthy model that is injected into the system to facilitate the detection of small fault . Since the auxiliary input signal generation leads to a non-convex optimization problem, it is transformed into a mixed integer quadratic programming problem. Finally, a case study based on a DC motor is used to show the effectiveness of the proposed method.

**KEYWORDS:**
active fault detection, small fault, interval uncertainty, zonotope, set-membership

## 1 | INTRODUCTION

In modern industries, operational safety and product quality of systems are important issues. If a fault occurs, it will not only affect the quality of the product, but it can also consequently bring security risks to the systems and operators. Therefore, fault diagnosis (FD)[1,2] plays a crucial role in industrial processes. Over the past decades, an important number of FD methods have been developed. These methods can be classified into passive[3] and active FD[4] depending if the system input is manipulated or not. In passive FD, the system is monitored using the system inputs and outputs without manipulation. Passive FD approaches can be divided into model-based methods[5,6], knowledge-based methods[7], and data-driven methods[8,9]. On the other hand, the key idea of active FD is to enhance the output separability of the healthy model from the faulty ones by manipulating the input signal[10]. In this way, the fault characteristics become more clearly such that smaller faults can be detected. For this reason, active FD has attracted increasing researcher attention in recent years. Active FD methods mainly include deterministic and probabilistic methods depending on the underlying assumptions regarding system noise and disturbance[11]. The deterministic methods assume that the noise and disturbance can be modeled as an unknown but bounded signal. Examples of such methods are the [illegible] which assume that uncertainties such as noise and disturbance affecting the system can be represented by random variables with known probability density functions. Then, fault detection is based on probabilistic methods such as statistical tests[14] or the Bayesian approach[15].

Most of the existing active FD methods assume that the noise and system disturbance follow a Gaussian distribution. However, such a prior knowledge of the probability distribution of the noise and disturbance in the actual system is difficult to be satisfied in practice [16]. On the other hand, the methods of guaranteed active FD generally do not assume any prior information regarding measurement noise and process disturbance distribution of the system except that they are unknown but the upper and lower bounds are known. Using this information and by designing auxiliary input signals in the appropriate manner, the output set of healthy model and the output set of faulty one can be separated improving the fault detection performance. Compared with other existing active FD methods, guaranteed active FD method is simpler and can detect smaller faults, attracting the attention of researchers in recent years. Guaranteed active FD mainly relies on the set-membership approach to bound the effect of the uncertainties of system on the system outputs/states. Set-membership approach can compute a set containing all the possible system outputs/states that are consistent with the unknown but bounded disturbances, modeling uncertainties and measurement noise. Hence, it is a suitable technique for state estimation when a system is modeled by some unknown but bounded disturbances. The set-membership approach considers the system disturbance and measurement noise bounded by means of a set. Several alternative set descriptions have been considered in the literature including ellipsoids, intervals, polytopes and zonotopes.

In the field of guaranteed active FD, elliposidal sets have been widely used for bounding uncertainty. For example, uncertainties such as measurement noise and process disturbance of system are expressed in ellipsoidal form. Then, active FD is realized by designing auxiliary input signals off-line [17] or on-line [18]. Compared with ellipsoids, zonotopes produces less conservative results when designing auxiliary input signals. Moreover, they can be used not only in the design of auxiliary input signals for open-loop systems [19], but also for closed-loop systems [20]. In addition, the idea of active FD based on set-membership approach is also used for active fault isolation [21] and multi-model separation [22].

Generally, the existing active FD methods based on the set-membership approach mainly use the idea of the set theory to bound system outputs using sets [23]. The observer design method can not only used to reduce the size of the system output sets but to guarantee the convergence. Therefore, in this paper, the zonotopic Kalman filter method is used, which reduces the size of the system output sets. It should be mentioned that the uncertain system contains not only process disturbance and measurement noise, but also the uncertainties of system parameters, increasing the size of the minimum detectable faults. However, to the best knowledge of the authors', little attention has been paid on active fault detection based on set-membership method for system with parametric uncertainty. In the work of Zhou [24], an interval fault estimation approach is proposed for discrete-time linear parameter-varying systems, however, it deals with the problem of passive fault detection. Motivated by the work [24], in our work, we mainly focused on designing a proper auxiliary input signal for discrete-time system with parametric uncertainties to reduce the size of the minimum detectable faults.

The main contributions of this paper can be summarized as follows: First, an active fault detection is proposed based on zonotopic Kalman filter observer for discrete-time system with bounded uncertainties. Following the earlier work regarding active fault diagnosis based on set-membership approach, we first apply this method to discrete-time system with parametric uncertainty, in which an auxiliary input signal is designed to separate the output zonotopes in the healthy case from the output zonotopes in the faulty case. Besides, in order to reduce the conservatism of auxiliary input signal design process, a zonotopic observer is designed to estimate the system output zonotope. Finally, the proposed approach is assessed using a case study based on a DC motor showing an improved detection in case of small faults.

The remainder of the paper is organized as follows. First, in Section 2, some preliminaries and the statement of the problem formulation used in this paper are introduced. Then, the zonotopic observer is designed to reduce the output set size in Section 3. An optimal auxiliary input signal is obtained by using output sets in Section 4. In Section 5, a DC motor is used as a case study and the simulation results show the effectiveness of the proposed method. Finally, the conclusion of this paper is introduced in Section 6.

## 2 | PRELIMINARIES AND PROBLEM FORMULATION

### 2.1 | Preliminaries

**Definition 1.** The $r$ order zonotope $\mathcal{Z}$ is defined as

$$\mathcal{Z} = p + \sum_{j=1}^{r} \alpha_j h_j = p \oplus H\mathbf{B}^r = \langle p, H \rangle, \tag{1}$$

where $p \in \mathbb{R}^n$ and $H = \{h_1, h_2, \cdots, h_r\} \in \mathbb{R}^{n\times r}$ are the center and the generator matrix of $\mathcal{Z}$, respectively. $\mathbf{B}^r = [-1, +1]^r$ is a unitary hypercube and $\|\alpha\|_\infty \leq 1$.

**Property 1.** Considering an interval $[a_1, a_2]$, mid $[a_1, a_2] = \frac{a_1+a_2}{2}$ and rad $[a_1, a_2] = \frac{a_2-a_1}{2}$ are the center and radius of the interval, respectively.

**Property 2.** Given an interval matrix $[A]$, where$A_{tj} = \{a_{tj} : a_{1,tj} \leq a_{tj} \leq a_{2,tj}\}$. The center and radius of the interval matrix are mid$[A]_{tj} = \frac{a_{1,tj}+a_{2,tj}}{2}$ and rad$[A]_{tj} = \frac{a_{2,tj}-a_{1,tj}}{2}$, respectively.

**Property 3.** The Minkowski sum of two zonotopes $\mathcal{Z}_1 = p_1 \oplus H_1\mathbf{B}^{r_1}$ and $\mathcal{Z}_2 = p_2 \oplus H_2\mathbf{B}^{r_2}$ is defined as

$$\mathcal{Z}_1 \oplus \mathcal{Z}_2 = \langle p_1, H_1\rangle \oplus \langle p_2, H_2\rangle = (p_1 + p_2) \oplus \begin{bmatrix} H_1 & H_2 \end{bmatrix} \mathbf{B}^{r_1+r_2}. \tag{2}$$

**Property 4.** The product of matrix $M$ and zonotope $\mathcal{Z} = \langle p, H\rangle$ is calculated as

$$M\mathcal{Z} = \langle Mp, MH\rangle. \tag{3}$$

**Property 5.** [25] Frobenius radius of the generator matrix $H$ can be used as an indicator to measure the size of the zonotope. It is expressed as

$$J = \sqrt{\text{tr}(H^T H)} = \sqrt{\text{tr}(HH^T)}, \tag{4}$$

where tr$(\cdot)$ is the matrix trace.

**Property 6.** [26] Considering a family of zonotopes represented by $\mathcal{Z} = p \oplus [H]\mathbb{B}^r$, where $p \in \mathbf{R}^n$ is a real vector, $[H] \in \mathbb{I}^{n\times r}$ is an interval matrix, $\mathbb{I}$ is defined as a set of real compact intervals. A family of zonotopes can be bounded by an outer approximation, as follows

$$\mathcal{Z} = p \oplus [\text{mid}[H] \;\; \text{rs}(\text{rad}[H])]\mathbf{B}^{r+n}. \tag{5}$$

where $\text{rs}(H) = \text{diag}(\sum_{j=1}^{r} |H_{n,j}|)$.

**Property 7.** [27] The product of an interval $[A]$ and a matrix $B$ denoted by $[A]B$ is bounded by a zonotope whose center and radius are mid $([A]\, B) = (\text{mid}\,[A])\, B$ and rad $([A]\, B) = (\text{mid}\,[A])\,|B|$, respectively. $|B|$ is the absolute value of each element in the matrix $B$.

**Lemma 1.** [28] A zonotope $\mathcal{Z}$ can be bounded by a minimal box $\square\mathcal{Z}$ known as interval hull

$$\mathcal{Z} \subset \square\mathcal{Z} = p \oplus \text{rs}(H)\mathbf{B}^r. \tag{6}$$

**Lemma 2.** [29] Let consider the $r$-order zonotope $\mathcal{Z} = p \oplus H\mathbf{B}^r \subset \mathbb{R}^n$ and the integer $n \leq s \leq r$. The column vector of the matrix $H$ is arranged in descending order of the Euclidean norm to obtain the matrix $\bar{H}$. $\mathcal{Z}$ can be included in a $s$-order $\bar{\mathcal{Z}}$, i.e.

$$\mathcal{Z} \subseteq \bar{\mathcal{Z}} = p \oplus \begin{bmatrix} \bar{H}_1 & Q \end{bmatrix} \mathbf{B}^s, \tag{7}$$

where $\bar{H}_1$ the first $s - n$ column vectors of $\bar{H}$, $\bar{H}_2$ the last $n$ column vectors of $\bar{H}$. $Q$ is the box containing $\bar{H}_2$ obtained by Lemma 1, i.e.

$$Q_{tt} = \sum_{j=1}^{r} |\bar{H}_2|_{tj}, t = 1, 2, \cdots, n. \tag{8}$$

**Lemma 3.** [30,31] Given two zonotopes $\mathcal{X} = \langle a_x + b_x, H_x\rangle$ and $\mathcal{Y} = \langle a_y + b_y, H_y\rangle$, $\mathcal{X} \bigcap \mathcal{Y} = \varnothing$ if and only if

$$a_y - a_x \notin \langle b_x, H_x\rangle \oplus \langle -b_y, H_y\rangle. \tag{9}$$

## 2.2 | Problem formulation

Let consider the class of uncertain discrete-time systems as:

$$\begin{cases} x_{k+1}^{[i]} = A^{[i]}(\theta)x_k^{[i]} + B^{[i]}u_k + B_\omega^{[i]}\omega_k^{[i]}, \\ y_k^{[i]} = C^{[i]}x_k^{[i]} + D_\upsilon^{[i]}\upsilon_k^{[i]}, \quad i = 0, 1, 2, \cdots, q, \end{cases} \tag{10}$$

where $i$ is the system model: the case $i = 0$ corresponds to the healthy model, otherwise, the other cases correspond to the faulty models, where $q$ denotes the total number of models. $x_k \in \mathbb{R}^{n_x}$, $u_k \in \mathbb{R}^{n_u}$,$y_k \in \mathbb{R}^{n_y}$ are state, input and output of the system at sample time $k$, respectively. $\omega_k \in \mathbb{R}^{n_\omega}$ and $\upsilon_k \in \mathbb{R}^{n_\upsilon}$ represent the process disturbance and measurement noise of the

system, respectively. $A^{[i]}(\theta)$, $B^{[i]}$, $C^{[i]}$, $B_{\omega}^{[i]}$, $D_{\upsilon}^{[i]}$ are matrices of appropriate dimensions. $\theta$ is a vector that contains the uncertain parameters of the system that are assumed to be unknown but bounded. $A(\theta)$ is an uncertain matrix that can be defined as an interval matrix $[A]$.

This paper assumes that the initial state, process disturbance and measurement noise of the system are unknown but bounded as follows

$$\begin{aligned} x_0^{[i]} &\in \mathcal{X}_0^{[i]} = \left\langle p_0^{[i]}, H_0^{[i]} \right\rangle, \\ \omega_k^{[i]} &\in \mathcal{W}^{[i]} = \left\langle 0, H_{\omega}^{[i]} \right\rangle, \\ \upsilon_k^{[i]} &\in \mathcal{V}^{[i]} = \left\langle 0, H_{\upsilon}^{[i]} \right\rangle, \end{aligned} \tag{11}$$

where $\mathcal{X}_0^{[i]}$, $\mathcal{W}^{[i]}$ and $\mathcal{V}^{[i]}$ are the zonotopes bounding the initial state, process disturbance and measurement noise, respectively. The output zonotopes of the system can be obtained by propagating the uncertainty using the zonotope properties and the system model (10).

*Remark 1.* As discussed in[32], because of the parametric uncertainty, process disturbances and noise, there will always be a minimum fault size that will be not be detectable (i.e., the measured output will be in the healthy output set $\mathcal{Y}^{[0]}$ even in the fault presence) or isolable (i.e., $\mathcal{Y}^{[i]} \cap \mathcal{Y}^{[j]} \neq \emptyset, i \neq j, i, j \in \{1, 2, \cdots, q\}$).

To reduce the size of the minimum detectable/isolable faults, active FD based on the auxiliary input signal design relies on designing an auxiliary input signal, and injecting it into the system to improve the fault separability. Active FD based on set-membership approaches aims at designing auxiliary input signals to separate the output sets of different models, i.e.

$$\mathcal{Y}^{[i]} \cap \mathcal{Y}^{[j]} = \emptyset, i \neq j, i, j \in \{0, 1, 2, \cdots, q\}, \tag{12}$$

where $\mathcal{Y}^{[i]}$ and $\mathcal{Y}^{[j]}$ are the output sets of model $i$ and model $j$, respectively.

Figure 1 shows the process of active fault detection based on set-membership method. The healthy output set and faulty output set when the auxiliary input signal is not added to the system are shown in Figure 1(a). When the healthy and faulty models intersect, it is impossible to judge whether the system is faulty or not. When the optimal auxiliary input signal is injected into the system, the two sets are separated as shown in Figure 1(b).

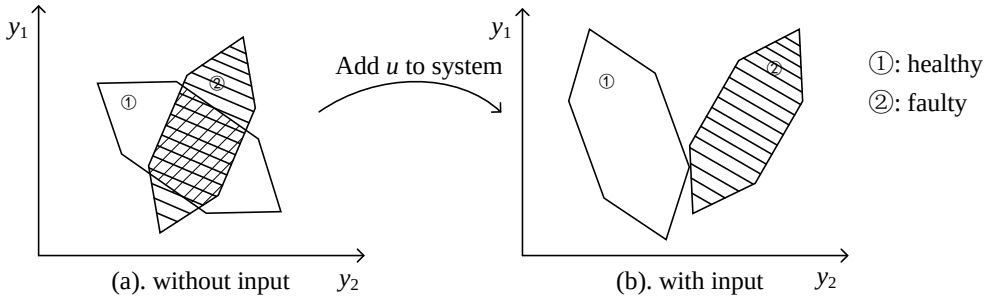


**FIGURE 1** Process of active fault detection.

The main objective of this paper is to design an optimal input signal such that the healthy output zonotope can be separated from the faulty output zonotope for discrete-time systems with parametric uncertainty.

## 3 | BOUNDING OUTPUT SET USING ZONOTOPIC OBSERVERS

The diagram of the approach proposed is this paper is depicted in Figure 2. In this figure, $u_{k-1}$ is the auxiliary input signal, $y_k$ is the system output, $\hat{x}_k^{[0]}$ and $\hat{x}_k^{[1]}$ are the state estimations obtained using the healthy and faulty models, respectively. $\mathcal{Y}_k^{[0]}$ and $\mathcal{Y}_k^{[1]}$ are the output zonotopes estimated using the healthy and faulty models, respectively. In order to reduce the conservativeness, a zonotopic observer is designed for estimating the output zonotope instead of using the systen model (10) as usually done in the active fault detection literature. Then, an auxiliary input signal is designed to separate the output zonotopes of the healthy model

from the output zonotopes of the faulty model. Finally, the input signal is injected into the system to obtain the fault detection results.

The state observer mainly corrects the state of the system using the error between the measured output and the observed output. Therefore, the size of the output set is tighter by using a state observer leading to less conservative results that using the system model (10). In this section, a zonotopic observer is first designed for (10). Then, the size of the output zonotopes is analyzed and it is demonstrated that the zonotope size can be reduced with the proposed observer-based design method.

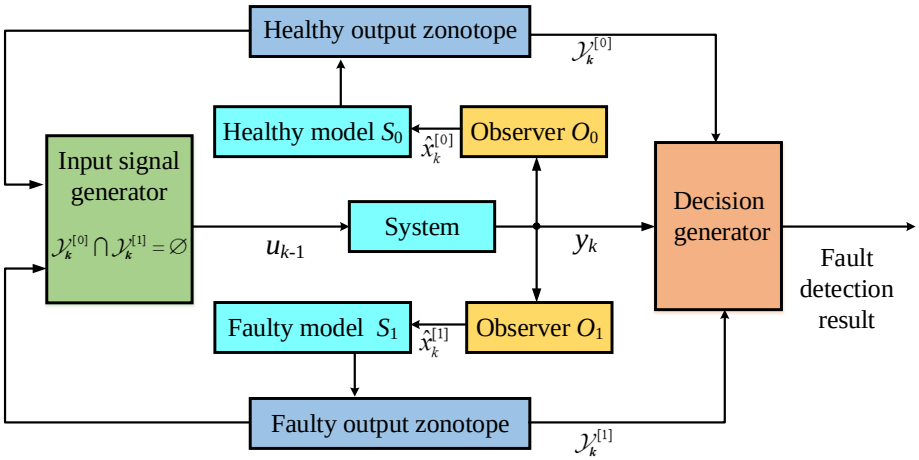


**FIGURE 2** Schematic diagram of the proposed approach.

## 3.1 | Zonotopic observer design

Based on the zonotopic Kalman filter approach[33], the observer for the system (10) has the following structure

$$\hat{x}_{k+1}^{[i]} = A^{[i]}(\theta)\hat{x}_k^{[i]} + B^{[i]}u_k + B_\omega^{[i]}\omega_k^{[i]} + L_k^{[i]}\left(y_k - C^{[i]}\hat{x}_k^{[i]} - D_\upsilon^{[i]}\upsilon_k^{[i]}\right), i = 0, 1, 2, \cdots, q. \tag{13}$$

where $\hat{x}_k^{[i]}$ is the estimate of the state at time $k$, $L_k^{[i]}$ is the time-varying observer gain and $y_k$ is the system output.

**Theorem 1.** Assume that the system state estimation at time sample $k$ satisfies $\hat{x}_k^{[i]} \in \mathcal{X}_k^{[i]} = \langle p_k^{[i]}, H_k^{[i]} \rangle$. Then, the state at sample time $k+1$ is given by

$$\hat{x}_{k+1}^{[i]} \in \mathcal{X}_{k+1}^{[i]} = \langle p_{k+1}^{[i]}, H_{k+1}^{[i]} \rangle, \tag{14}$$

where

$$\begin{cases} p_{k+1}^{[i]} = \mathrm{mid}([A^{[i]}] - L_k^{[i]}C^{[i]})p_k^{[i]} + B^{[i]}u_k + L_k{}^{[i]}y_k \\ H_{k+1}^{[i]} = \left[\mathrm{mid}([A^{[i]}] - L_k^{[i]}C^{[i]})\bar{H}_k^{[i]} \quad \mathrm{rs}(\mathrm{rad}([A^{[i]}] - L_k^{[i]}C^{[i]})\left|\bar{H}_k^{[i]}\right|),\right. \\ \qquad \left.\mathrm{rs}(\mathrm{rad}([A^{[i]}] - L_k^{[i]}C^{[i]})\left|p_k^{[i]}\right|) \quad B_\omega^{[i]}H_\omega^{[i]} \quad L_k^{[i]}D_\upsilon^{[i]}H_\upsilon^{[i]}\right], \end{cases} \tag{15}$$

$p_{k+1}^{[i]} \in \mathbb{R}_x^n$, $H_{k+1}^{[i]} \in \mathbb{R}^{n_x \times r_x}$, $\bar{H}_{k+1}^{[i]}$ represents the generator matrix after the zonotope reduction using Lemma 2 at sample time $k+1$.

*Proof.* According to (13) and taking into account the noise and disturbances bounds (11), the zonotope $\mathcal{X}_{k+1}^{[i]}$ can be rewritten as

$$\begin{aligned}\hat{x}_{k+1}^{[i]} \in \mathcal{X}_{k+1}^{[i]} =&[A^{[i]}]\mathcal{X}_k^{[i]} \oplus B^{[i]}u_k \oplus B_\omega^{[i]}\mathcal{W}^{[i]} \oplus L_k^{[i]}y_k \oplus (-L_k^{[i]}\mathcal{X}_k^{[i]}) \oplus (-L_k^{[i]}D_\upsilon^{[i]}\mathcal{V}^{[i]})\\ =&\left[([A^{[i]}]-L_k^{[i]}C^{[i]}) \odot \left\langle p_k^{[i]}, H_k^{[i]}\right\rangle\right] \oplus B^{[i]}u_k\\ &\oplus L_k^{[i]}y_k \oplus \left[B_\omega^{[i]} \odot \left\langle 0, H_\omega^{[i]}\right\rangle\right] \oplus \left[(-L_k^{[i]}D_\upsilon^{[i]}) \odot \left\langle 0, H_\upsilon^{[i]}\right\rangle\right]\\ =&(([A^{[i]}]-L_k^{[i]}C^{[i]})p_k^{[i]} + B^{[i]}u_k + L_k^{[i]}y_k)\\ &\oplus \left[([A^{[i]}]-L_k^{[i]}C^{[i]})H_k^{[i]} \;\; B_\omega^{[i]}H_\omega^{[i]} \;\; L_k^{[i]}D_\upsilon^{[i]}H_\upsilon^{[i]}\right].\end{aligned} \tag{16}$$

Using properties of the zonotope and Lemma 2, the center of the state zonotope and the generator matrix can be obtained at sample time $k+1$. □

In this paper, we mainly will use the output set that is consistent with the unknown but bounded parametric uncertainty, disturbances and noise. Then, from the zonotope that bounds the states (14), the zonotope that bounds the estimated output $\mathcal{Y}_{k+1}^{[i]}$ can be obtained using (13) as follows

$$\begin{aligned}y_{k+1}^{[i]} \in \mathcal{Y}_{k+1}^{[i]} &= C^{[i]}\mathcal{X}_{k+1}^{[i]} \oplus D_\upsilon^{[i]}\mathcal{V}^{[i]}\\ &= \left[C^{[i]} \odot \left\langle p_{k+1}^{[i]}, H_{k+1}^{[i]}\right\rangle\right] \oplus \left[D_\upsilon^{[i]} \odot \left\langle 0, H_\omega^{[i]}\right\rangle\right]\\ &= \left\langle C^{[i]}p_{k+1}^{[i]}, \left[C^{[i]}H_{k+1}^{[i]} \;\; D_\upsilon^{[i]}H_\upsilon^{[i]}\right]\right\rangle.\end{aligned} \tag{17}$$

Therefore, the center and radius of output zonotope can be obtained

$$\begin{cases} p_{y,k+1}^{[i]} = C^{[i]}p_{k+1}^{[i]},\\ H_{y,k+1}^{[i]} = \left[C^{[i]}H_{k+1}^{[i]} \;\; D_\upsilon^{[i]}H_\upsilon^{[i]}\right], \end{cases} \tag{18}$$

where $p_{y,k+1}^{[i]} \in \mathbb{R}^{n_y}$, $H_{y,k+1}^{[i]} \in \mathbb{R}^{n_y \times r_y}$.

According to[28], given an observer such as (13), the optimal time-varying gain that minimizes the size of zonotope, measured by means of the Frobenius norm of the zontope segment matrix as

$$(J_k^{[i]})^2 = \mathrm{tr}((H_{k+1}^{[i]})^T H_{k+1}^{[i]}), \tag{19}$$

can be obtained as follows

$$\begin{aligned} L_k^{[i]} &= \mathrm{mid}([A^{[i]}])K_k^{[i]},\\ K_k^{[i]} &= G_k^{[i]}(S_k^{[i]})^{-1},\\ G_k^{[i]} &= P_k^{[i]}(C^{[i]})^T,\\ S_k^{[i]} &= C^{[i]}P_k^{[i]}(C^{[i]})^T + Q_\upsilon^{[i]},\\ P_k^{[i]} &= \bar{H}_k^{[i]}(\bar{H}_k^{[i]})^T,\\ Q_\upsilon^{[i]} &= D_\upsilon^{[i]}H_\upsilon^{[i]}(H_\upsilon^{[i]})^T(D_\upsilon^{[i]})^T. \end{aligned} \tag{20}$$

The optimal gain (20) is derived considering that the size of the output zonotope (19) is minimized when $\frac{\partial (J_k^{[i]})^2}{\partial L_k^{[i]}} = 0$ based on the results in Combastel[34].

## 3.2 | Analysis of the size of output zonotopes

As previously discussed, the reduction of the size of the minimum detectable/isolable faults can be achieved by means of the design of the adequate auxiliary input signal such that the output zonotopes of the different models do not overlap. However, when the overlapping is important, the size of the auxiliary input signal to be used should be large to separate the output zonotope ofthe different models, disturbing the desired behaviour of the system. Therefore, in order to obtain a small auxiliary input signal, the size of the output zonotope should be as smaller as possible.

**Theorem 2.** Consider the system (10). The size of the output zonotope at time $k+1$, measured by means of (19), using the observer (13) with optimal gain (20) is smaller than the output zonotope obtained directly using the system model (10),

$$J_{k+1} \leq \tilde{J}_{k+1}, \tag{21}$$

where $J_{k+1}$ and $\tilde{J}_{k+1}$ denote respectively the size of the output zonotope with and without observer.

*Proof.* The size of the output zonotope obtained with the observer can be measured by means of the Frobenius norm of the zonotope segment matrix (Property 5)

$$\begin{aligned}(J_{k+1})^2 =&\mathrm{tr}((H^{[i]}_{y,k+1})^T H^{[i]}_{y,k+1}) = \mathrm{tr}((\mathrm{mid}([A^{[i]}] - L^{[i]}_k C^{[i]})H^{[i]}_k)^T \mathrm{mid}([A^{[i]}] - L^{[i]}_k C^{[i]})H^{[i]}_k \\ &+ (\mathrm{rs}(\mathrm{rad}([A^{[i]}] - L^{[i]}_k C^{[i]}) \left|H^{[i]}_k\right|))^T \mathrm{rs}(\mathrm{rad}([A^{[i]}] - L^{[i]}_k C^{[i]}) \left|H^{[i]}_k\right|) \\ &+ (\mathrm{rs}(\mathrm{rad}([A^{[i]}] - L^{[i]}_k C^{[i]}) \left|p^{[i]}_k\right|))^T \mathrm{rs}(\mathrm{rad}([A^{[i]}] - L^{[i]}_k C^{[i]}) \left|p^{[i]}_k\right|) \\ &+ (B^{[i]}_\omega H^{[i]}_\omega)^T B^{[i]}_\omega H^{[i]}_\omega + (L^{[i]}_k D^{[i]}_\upsilon H^{[i]}_\upsilon)^T L^{[i]}_k D^{[i]}_\upsilon H^{[i]}_\upsilon).\end{aligned} \tag{22}$$

Using the properties of interval matrices, it follows that

$$\begin{aligned}&\mathrm{mid}([A^{[i]}] - L^{[i]}_k C^{[i]}) = \mathrm{mid}([A^{[i]}]) - L^{[i]}_k C^{[i]}, \\ &\mathrm{rad}([A^{[i]}] - L^{[i]}_k C^{[i]}) = \mathrm{rad}([A^{[i]}]).\end{aligned} \tag{23}$$

Therefore,

$$\begin{aligned}&(\mathrm{mid}([A^{[i]}] - L^{[i]}_k C^{[i]})H^{[i]}_k)^T \mathrm{mid}([A^{[i]}] - L^{[i]}_k C^{[i]})H^{[i]}_k \\ =&(H^{[i]}_k)^T (\mathrm{mid}([A^{[i]}]) - L^{[i]}_k C^{[i]})^T (\mathrm{mid}([A^{[i]}]) - L^{[i]}_k C^{[i]})H^{[i]}_k \\ =&(H^{[i]}_k)^T (\mathrm{mid}([A^{[i]}]))^T \mathrm{mid}([A^{[i]}])H^{[i]}_k - (H^{[i]}_k)^T (L^{[i]}_k C^{[i]})^T \mathrm{mid}([A^{[i]}])H^{[i]}_k \\ &- (H^{[i]}_k)^T (\mathrm{mid}([A^{[i]}]))^T L^{[i]}_k C^{[i]} H^{[i]}_k + (H^{[i]}_k)^T (L^{[i]}_k C^{[i]})^T L^{[i]}_k C^{[i]} H^{[i]}_k.\end{aligned} \tag{24}$$

We can proceed similarly to measure the size of output zonotope without observer

$$\begin{aligned}&(\tilde{J}_{k+1})^2 = \mathrm{tr}((\tilde{H}^{[i]}_{y,k+1})^T \tilde{H}^{[i]}_{y,k+1}) \\ =&\mathrm{tr}((\mathrm{mid}([A^{[i]}])\tilde{H}^{[i]}_k)^T \mathrm{mid}([A^{[i]}])\tilde{H}^{[i]}_k + (\mathrm{rs}(\mathrm{rad}([A^{[i]}]) \left|\tilde{H}^{[i]}_k\right|))^T \mathrm{rs}(\mathrm{rad}([A^{[i]}]) \left|\tilde{H}^{[i]}_k\right|) \\ &+ (\mathrm{rs}(\mathrm{rad}([A^{[i]}]) \left|\tilde{p}^{[i]}_k\right|))^T \mathrm{rs}(\mathrm{rad}([A^{[i]}]) \left|\tilde{p}^{[i]}_k\right|) + (B^{[i]}_\omega H^{[i]}_\omega)^T B^{[i]}_\omega H^{[i]}_\omega).\end{aligned} \tag{25}$$

In order to verify the size of output zonotope obtained by means of the observer (13) is smaller, the difference between (22) and (25) is evaluated

$$\begin{aligned}(J_{k+1})^2 - (\tilde{J}_{k+1})^2 =&\mathrm{tr}((L^{[i]}_k C^{[i]} H^{[i]}_k)^T L^{[i]}_k C^{[i]} H^{[i]}_k - (\mathrm{mid}([A^{[i]}])H^{[i]}_k)^T L^{[i]}_k C^{[i]} H^{[i]}_k \\ &- (L^{[i]}_k C^{[i]} H^{[i]}_k)^T \mathrm{mid}([A^{[i]}])H^{[i]}_k + (L^{[i]}_k D^{[i]}_\upsilon H^{[i]}_\upsilon)^T L^{[i]}_k D^{[i]}_\upsilon H^{[i]}_\upsilon).\end{aligned} \tag{26}$$

Considering the observer optimal gain (20), previous equation can be rewritten

$$(J_{k+1})^2 - (\tilde{J}_{k+1})^2 = -\mathrm{tr}(L^{[i]}_k C^{[i]} H^{[i]}_k (H^{[i]}_k)^T (C^{[i]})^T (L^{[i]}_k)^T) - \mathrm{tr}(L^{[i]}_k Q^{[i]}_\upsilon (L^{[i]}_k)^T), \tag{27}$$

where $Q^{[i]}_\upsilon = D^{[i]}_\upsilon H^{[i]}_\upsilon (D^{[i]}_\upsilon H^{[i]}_\upsilon)^T$.

Since $L^{[i]}_k C^{[i]} H^{[i]}_k (H^{[i]}_k)^T (C^{[i]})^T (L^{[i]}_k)T$ and $L^{[i]}_k Q^{[i]}_\upsilon (L^{[i]}_k)^T$ are symmetric matrices with positive elements, it follows that

$$(J_{k+1})^2 - (\tilde{J}_{k+1})^2 \leq 0, \tag{28}$$

Therefore, Theorem 2 is proved. □

In summary, since the size of the output zonotope is reduced by using an observer-based method, the auxiliary input signal designed by the optimal zonotopic observer method will be smaller. The optimal input signal will be obtained by forcing that the intersection of the output zonotopes in the different system modes is empty. The injection of this signal into the system will allow reducing the size of the minimum separable faults.

## 4 | OPTIMAL AUXILIARY INPUT DESIGN

In this section, an optimal auxiliary input signal is designed by using the output sets determined in previous section. Since the addition of the input signal will affect the system, the input signal is required to be minimized such that small faults could be

detected. In this section, the problem of solving the optimal auxiliary input signal design is mainly transformed into the problem of solving the mixed integer quadratic programming (MIQP).

The optimal auxiliary input signal should satisfy

$$\begin{aligned} &\min_{u_k} (u_k)^T R u_k \\ &s.t. \quad \mathcal{Y}_{k+1}^{[i]} \cap \mathcal{Y}_{k+1}^{[j]} = \varnothing, i \neq j, i, j \in \{0, 1, 2, \cdots, q\}. \end{aligned} \tag{29}$$

where $R$ is a positive semi-definite matrix.

According to (18), the output zonotope is given by

$$\begin{aligned} \mathcal{Y}_{y,k+1}^{[i]} &= \left\langle p_{y,k+1}^{[i]}, H_{y,k+1}^{[i]} \right\rangle \\ &= C^{[i]}([A^{[i]}] - L_k^{[i]} C^{[i]}) \mathcal{X}_k^{[i]} \oplus C^{[i]} B^{[i]} u_k \oplus C^{[i]} L_k^{[i]} y_k \oplus C^{[i]} B_\omega^{[i]} \mathcal{W}^{[i]} \oplus (-C^{[i]} L_k^{[i]} D_v^{[i]} \mathcal{V}^{[i]}). \end{aligned} \tag{30}$$

that can be expressed as

$$\mathcal{Y}_{k+1}^{[i]} = \mathcal{M}_k^{[i]} + C^{[i]} B^{[i]} u_k = \left\langle \bar{p}_{y,k+1}^{[i]} + C^{[i]} B^{[i]} u_k, H_{y,k+1}^{[i]} \right\rangle, \tag{31}$$

with

$$\mathcal{M}_k^{[i]} = \left\langle \bar{p}_{y,k+1}^{[i]}, H_{y,k+1}^{[i]} \right\rangle, \tag{32}$$

where

$$\begin{aligned} \bar{p}_{y,k+1}^{[i]} &= C^{[i]} \mathrm{mid}([A^{[i]}] - L_k^{[i]} C^{[i]}) p_k^{[i]} + L_k{}^{[i]} y_k, \\ p_{y,k+1}^{[i]} &= \bar{p}_{y,k+1}^{[i]} + C^{[i]} B^{[i]} u_k. \end{aligned} \tag{33}$$

**Theorem 3.** The intersection of output zonotopes of the healthy and faulty models is empty

$$\mathcal{Y}_{k+1}^{[i]} \cap \mathcal{Y}_{k+1}^{[j]} = \varnothing, i \neq j, i, j \in \{0, 1, 2, \cdots, q\}. \tag{34}$$

if and only if

$$\triangle^{[ij]} u_k \notin \mathcal{Y}_{m,k}^{[ij]}, \tag{35}$$

where $\triangle^{[ij]} = C^{[j]} B^{[j]} - C^{[i]} B^{[i]}$, $\mathcal{Y}_{m,k}^{[ij]} = \mathcal{M}_k^{[i]} - \mathcal{M}_k^{[j]}$.

*Proof.* Using (32), (34) can be written as

$$\left\langle \bar{p}_{y,k+1}^{[i]} + C^{[i]} B^{[i]} u_k, H_{y,k+1}^{[i]} \right\rangle \cap \left\langle \bar{p}_{y,k+1}^{[j]} + C^{[j]} B^{[j]} u_k, H_{y,k+1}^{[j]} \right\rangle = \varnothing. \tag{36}$$

According to Lemma 3, if and only if

$$C^{[j]} B^{[j]} u_k - C^{[i]} B^{[i]} u_k \notin \left\langle \bar{p}_{y,k+1}^{[i]}, H_{y,k+1}^{[i]} \right\rangle \oplus \left\langle \bar{p}_{y,k+1}^{[j]}, H_{y,k+1}^{[j]} \right\rangle = \mathcal{M}_k^{[i]} - \mathcal{M}_k^{[j]}. \tag{37}$$

Theorem 3 is proved. □

So, according to Theorem 3, (29) can be rewritten as

$$\begin{aligned} &\min_{u_k} (u_k)^T R u_k \\ &s.t. \quad \triangle^{[ij]} u_k \notin \mathcal{Y}_{m,k}^{[ij]}, i \neq j, i, j \in \{0, 1, 2, \cdots, q\}. \end{aligned} \tag{38}$$

Since optimization problem (38) is a non-convex optimization problem, it is not easy to obtain the optimal solution. So, the optimization problem (38) is reformulated and transformed into a MIQP problem to obtain the effective solution.

To this aim, the zonotope $\mathcal{Y}_{m,k}^{[ij]}$ is defined as

$$\mathcal{Y}_{m,k}^{[ij]} = \left\langle p_{m,k}^{[ij]}, H_{m,k}^{[ij]} \right\rangle, \tag{39}$$

where $p_{m,k}^{[ij]} \in \mathbb{R}^{[n_y]}$, $H_{m,k}^{[ij]} \in \mathbb{R}^{n_y \times 2r_y}$. When $H_{m,k}^{[ij]}$ is a row full rank matrix, $\mathcal{Y}_{m,k}^{[ij]}$ is a non-empty set.

Using Definition 1, when $\triangle^{[ij]} u_k \in \mathcal{Y}_{m,k}^{[ij]}$,

$$\triangle^{[ij]} u_k = p_{m,k}^{[ij]} + H_{m,k}^{[ij]} \alpha'^{[ij]}, \tag{40}$$

where $\left\|\alpha'^{[ij]}\right\|_\infty \leq 1$. If $\triangle^{[ij]}u_k \notin \mathcal{Y}_{m,k}^{[ij]}$,

$$\triangle^{[ij]}u_k = p_{m,k}^{[ij]} + H_{m,k}^{[ij]}\alpha^{[ij]}, \tag{41}$$

where $\left\|\alpha^{[ij]}\right\|_\infty \leq 1 + \varepsilon^{[ij]}$ and $\varepsilon^{[ij]} > 0$.

Therefore, (34) can be rewritten as

$$\begin{aligned}
&\min_{u_k} (u_k)^T R u_k \\
&\min_{\varepsilon^{[ij]},\alpha^{[ij]}} \varepsilon^{[ij]} \\
&s.t. \quad \triangle^{[ij]}u_k = H_{m,k}^{[ij]}\alpha^{[ij]} + p_{m,k}^{[ij]}, \\
&\qquad \left\|\alpha^{[ij]}\right\|_\infty \leq 1 + \varepsilon^{[ij]}, \\
&\qquad \varepsilon^{[ij]} > 0, \quad i \neq j, i, j \in \{0, 1, 2, \cdots, q\}.
\end{aligned} \tag{42}$$

Note that the feasible set in (34) is an unbounded set due to the constraint $\varepsilon^{[ij]} > 0$ in (42). Therefore, in order to obtain the optimal auxiliary input signal $u_k$, suppose there is an upper bound $\bar{\varepsilon}^{[ij]}$ and a lower bound $\underline{\varepsilon}^{[ij]}$, i.e.

$$\underline{\varepsilon}^{[ij]} \leq \varepsilon^{[ij]} \leq \bar{\varepsilon}^{[ij]}. \tag{43}$$

where $\underline{\varepsilon}^{[ij]} > 0$ and $\bar{\varepsilon}^{[ij]}$ are established according to the physical knowledge of the particular system.

Using (43), (42) can be rewritten as the following two-layer optimization problem

$$\begin{aligned}
&\min_{u_k} (u_k)^T R u_k \\
&\min_{\varepsilon^{[ij]},\alpha^{[ij]}} \varepsilon^{[ij]} \\
&s.t. \quad \underline{\varepsilon}^{[ij]} \leq \varepsilon^{[ij]} \leq \bar{\varepsilon}^{[ij]}, \\
&\qquad \triangle^{[ij]}u_k = H_{m,k}^{[ij]}\alpha^{[ij]} + p_{m,k}^{[ij]}, \\
&\qquad \left\|\alpha^{[ij]}\right\|_\infty \leq 1 + \varepsilon^{[ij]}, \\
&\qquad \varepsilon^{[ij]} > 0, \quad i \neq j, i, j \in \{0, 1, 2, \cdots, q\}.
\end{aligned} \tag{44}$$

This two-layer optimization problem is not easy to be solved. Using the Theorem 3.3.1 and Theorem 3.4.1 in the book[35], the two-layer optimization problem in (44) can be transformed into a single-layer optimization problem by constructing a Lagrangian function.

**Theorem 4.** For system (10) and using the zonotopic observer in Theorem 1, the optimal auxiliary input signal can be obtained by solving the following optimization problem

$$\begin{aligned}
&\min_{u_k} (u_k)^T R u_k \\
&s.t. \quad \underline{\varepsilon}^{[ij]} \leq \varepsilon^{[ij]} \leq \bar{\varepsilon}^{[ij]}, \\
&\qquad \triangle^{[ij]}u_k = H_{m,k}^{[ij]}\alpha^{[ij]} + p_{m,k}^{[ij]}, \\
&\qquad \left\|\alpha^{[ij]}\right\|_\infty \leq 1 + \varepsilon^{[ij]}, \\
&\qquad (\mu_1^{[ij]} + \mu_2^{[ij]})^T \mathbf{1}{=}1, \\
&\qquad \mu_1^{[ij]} - \mu_2^{[ij]} = (H_{m,k}^{[ij]})^T \lambda^{[ij]}, \\
&\qquad (\alpha^{[ij]} - 1 - \varepsilon_l^{[ij]}) \in [-2(1 + \bar{\varepsilon}^{[ij]})(1 - b_{1,l}^{[ij]}), 0], \\
&\qquad (\alpha^{[ij]} + 1 + \varepsilon_l^{[ij]}) \in [0, 2(1 + \bar{\varepsilon}^{[ij]})(1 - b_{2,l}^{[ij]})], \\
&\qquad l = 1, 2, \cdots, 2r_y, \varepsilon^{[ij]} > 0, \ i \neq j, i, j \in \{0, 1, 2, \cdots, q\}.
\end{aligned} \tag{45}$$

where $\lambda^{[ij]}$, $\mu_1^{[ij]}$ and $\mu_2^{[ij]}$ are the Lagrange multipliers, vector $\mathbf{1}{=}\begin{bmatrix}1 & 1 & \cdots & 1\end{bmatrix} \in \mathbb{R}^{2r_y}$, $b_{1,l}^{[ij]}$ and $b_{2,l}^{[ij]}$ are binary variables. $\mu_1^{[ij]}$ and $\mu_2^{[ij]}$ respectively satisfy

$$\boldsymbol{\mu}_1^{[ij]} = \begin{bmatrix}\mu_{1,1}^{[ij]} & \mu_{1,2}^{[ij]} & \cdots & \mu_{1,2r_y}^{[ij]}\end{bmatrix}^{\mathrm{T}} \in \mathbb{R}^{2r_y}, \tag{46}$$

and

$$\boldsymbol{\mu}_2^{[ij]} = \left[\mu_{2,1}^{[ij]}\ \mu_{2,2}^{[ij]}\ \cdots\ \mu_{2,2r}^{[ij]}\right]^{\mathrm{T}} \in \mathbb{R}^{2r_y}, \tag{47}$$

*Proof.* The Lagrange function for the optimization problem (45) is

$$\begin{aligned}\mathcal{L} =&\varepsilon^{[ij]} + \lambda^{[ij]}(H_{m,k}^{[ij]}\alpha^{[ij]} + p_{m,k}^{[ij]} - \triangle^{[ij]}u_k) + \mu_{1,1}^{[ij]}(-\alpha_1^{[ij]} - 1 - \varepsilon^{[ij]}) + \mu_{1,2}^{[ij]}(-\alpha_2^{[ij]} - 1 - \varepsilon^{[ij]}) + \cdots\\ &+ \mu_{2,2r_y}^{[ij]}(-\alpha_{2r_y}^{[ij]} - 1 - \varepsilon^{[ij]}) + \mu_{1,1}^{[ij]}(\alpha_1^{[ij]} - 1 - \varepsilon^{[ij]}) + \mu_{2,2}^{[ij]}(\alpha_2^{[ij]} - 1 - \varepsilon^{[ij]}) + \cdots + \mu_{2,2r_y}^{[ij]}(\alpha_{2r_y}^{[ij]} - 1 - \varepsilon^{[ij]})\\ =&\varepsilon^{[ij]} + \lambda^{[ij]}(H_{m,k}^{[ij]}\alpha^{[ij]} + p_{m,k}^{[ij]} - \triangle^{[ij]}u_k) - (\mu_1^{[ij]})^T\alpha^{[ij]} - (\mu_1^{[ij]})^T\mathbf{1} - (\mu_1^{[ij]})^T\mathbf{1}\varepsilon^{[ij]}\\ &+ (\mu_2^{[ij]})^T\alpha^{[ij]} - (\mu_2^{[ij]})^T\mathbf{1} - (\mu_2^{[ij]})^T\mathbf{1}\varepsilon^{[ij]}.\end{aligned} \tag{48}$$

The first-order optimally conditions can be obtained by computing the derivative of $\mathcal{L}$ with respect the decision variables

$$\begin{aligned}&\frac{\partial\mathcal{L}}{\partial\varepsilon^{[ij]}} = 1 - (\mu_1^{[ij]} + \mu_2^{[ij]})^T\mathbf{1} = 0,\\ &\frac{\partial\mathcal{L}}{\partial\varepsilon^{[ij]}} = (H_{m,k}^{[ij]})^T - \mu_1^{[ij]} + \mu_2^{[ij]} = 0,\\ &\mu_{1,l}^{[ij]}(\alpha_l^{[ij]} - 1 - \varepsilon^{[ij]})=0,\\ &\mu_{2,l}^{[ij]}(\alpha_1^{[ij]} + 1 + \varepsilon^{[ij]}) = 0.\end{aligned} \tag{49}$$

The constraints $\mu_{1,l}^{[ij]}(\alpha_l^{[ij]} - 1 - \varepsilon^{[ij]}) = 0$ and $\mu_{2,l}^{[ij]}(\alpha_l^{[ij]} + 1 + \varepsilon^{[ij]}) = 0$ are reformulated by introducing binary variables $b_1^{[ij]}, b_2^{[ij]} \in \{0, 1\}$ as follows

$$\begin{aligned}&b_{1,l}^{[ij]} = 1 \Rightarrow \mu_{1,l}^{[ij]}, \text{free}, \quad (\alpha^{[ij]} - 1 - \varepsilon_l^{[ij]}) = 0,\\ &b_{1,l}^{[ij]} = 0 \Rightarrow \mu_{1,l}^{[ij]} = 0, \quad (\alpha^{[ij]} - 1 - \varepsilon_l^{[ij]}), \text{free},\\ &b_{2,l}^{[ij]} = 1 \Rightarrow \mu_{2,l}^{[ij]}, \text{free}, \quad (\alpha^{[ij]} + 1 + \varepsilon_l^{[ij]}) = 0,\\ &b_{2,l}^{[ij]} = 0 \Rightarrow \mu_{2,l}^{[ij]} = 0, \quad (\alpha^{[ij]} + 1 + \varepsilon_l^{[ij]}), \text{free}.\end{aligned} \tag{50}$$

Therefore, (50) can be written as

$$\begin{aligned}&\mu_{1,l}^{[ij]}\ ,\ \mu_{2,l}^{[ij]} \in [0, 1],\\ &(\alpha^{[ij]} - 1 - \varepsilon_l^{[ij]}) \in [-2(1 + \bar{\delta}^{[ij]}), 0],\\ &(\alpha^{[ij]} + 1 + \varepsilon_l^{[ij]}) \in [0, 2(1 + \bar{\delta}^{[ij]})],\end{aligned} \tag{51}$$

that after some manipulation can be expressed as the following linear constraints:

$$\begin{aligned}&\mu_{1,l}^{[ij]} \le b_{1,l}^{[ij]}\ ,\ \mu_{2,l}^{[0i]} \le b_{2,l}^{[ij]},\\ &(\alpha^{[ij]} - 1 - \varepsilon_l^{[ij]}) \in [-2(1 + \bar{\varepsilon}^{[ij]})(1 - b_{1,l}^{[ij]}), 0],\\ &(\alpha^{[ij]} + 1 + \varepsilon_l^{[ij]}) \in [0, 2(1 + \bar{\varepsilon}^{[ij]})(1 - b_{2,l}^{[ij]})].\end{aligned} \tag{52}$$

More details of this proof process can be seen in the Scott's work[30]. □

$\mathcal{V}^{[i]} = \left\langle 0, H_v^{[i]} \right\rangle, i = 0, 1, \cdots, q;$

*Remark 2.* Assume that the system is stable similarly as considered in the Zhai's and Scott's works[17,30]. Thus, an additional input signal, auxiliary input will not affect the stability of the system.

When the auxiliary input signal is obtained, the logic of active FD is mainly based on determining whether the output of the actual system is faulty, then the problem can be transformed into:

$$\text{Fault detection results} = \begin{cases} 1 & y_k \in \mathcal{Y}_k^{[0]},\\ -1 & y_k \in \mathcal{Y}_k^{[i]},\\ 0 & y_k \notin \mathcal{Y}_k^{[0]} \text{ and } y_k \notin \mathcal{Y}_k^{[i]}. \end{cases} \tag{53}$$

where $\mathcal{Y}_k^{[0]}$ and $\mathcal{Y}_k^{[i]}$ correspond to the output zonotopes in healthy and faulty models, respectively. If $y_k$ is inside the healthy output zonotope, we use 1 to represent the fault detection result, which means that the system is healthy operation. If $y_k$ falls into faulty output zonotope, $-1$ is used to represent that the system is faulty. However, sometimes the system is in the transient

**Algorithm 1** Active fault detection based on zonotope for uncertain systems

Given $A^{[i]}(\theta)$, $B^{[i]}$, $C^{[i]}$, $B_{\omega}^{[i]}$, $D_{v}^{[i]}$, $\mathcal{W}^{[i]}$ and $\mathcal{V}^{[i]}$, $i = 0, 1, \cdots, q$;
$\mathcal{X}_{k-1}^{[i]} \Leftarrow \mathcal{X}_{0}^{[i]}$, $y_{k-1} \Leftarrow y_0$;
**for** $k = 1$ to end **do**
  Obtain the optimal observer gain $L_{k-1}^{[i]}$;
  Compute $p_{m,k-1}^{[0i]}$ and $H_{m,k-1}^{[0i]}$ according to (32);
  Obtain $u_{k-1}$ by the Theorem 4, than inject it into the system (10);
  Measure $y_k$;
  Compute the healthy output zonotope $\mathcal{Y}_k^{[0]}$ and the faulty output zonotope $\mathcal{Y}_k^{[i]}$ of system respectively by using (17);
  **if** $y_k \in \mathcal{Y}_k^{[0]}$ **then**
    Fault detection results = 1, the system is healthy;
    **if** $y_k \in \mathcal{Y}_k^{[1]}$ **then**
      Fault detection results =-1, the system is faulty;
    **else**
      Fault detection results = 0, it can not be decided whether the system is faulty or not.
    **end if**
  **end if**
**end for**

state from healthy to faulty, $y_k$ belongs neither to the healthy output zonotope nor the faulty output zonotope at a particular time instant. Consequently, it can not be decided whether the system is faulty or not, we use 0 to represent this situation.

*Remark 3.* Assuming that there is a point $x \in \mathbb{R}^n$ and zonotope $\mathcal{X} = p \oplus H\mathbf{B}^r$, where $p \in \mathbb{R}^n$, $H \in \mathbb{R}^{n\times r}$. According to the properties of zonotope, the problem of determining whether a point belongs to a zonotope can be transformed into the following constraints:

$$\begin{cases} p_1 + H_1\alpha = x_1, \\ p_2 + H_2\alpha = x_2, \\ \quad\vdots \\ p_n + H_n\alpha = x_{n_x}, \end{cases} \tag{54}$$

where $\alpha$=$[\alpha_1 \ \alpha_2 \ \cdots \ \alpha_r]^T$ . Constraints (54) hold if and only if $\|\alpha_r\| \leq 1$. So, when $x$ satisfies the constraints (54), it means that $x$ belongs to the zonotope $\mathcal{X}$.

Thus, according to Remark 4, the verification of the fault detection conditions presented in (53) can be implemented by solving the constraint satisfaction problem (54). As a result, the proposed active FD method is summarized in Algorithm 1.

## 5 | SIMULATION

The low-frequency linear model of a permanent magnet DC motor[30] is used to verify the effectiveness of the proposed method in this paper. The expression of the model is as follows

$$\begin{aligned} \begin{bmatrix} \frac{di_m(t)}{dt} \\ \frac{dn_m(t)}{dt} \end{bmatrix} &= \begin{bmatrix} -\frac{R}{L} & -\frac{M_e}{L} \\ \frac{M_t}{J_1} & -\frac{f_r}{J_1} \end{bmatrix} \begin{bmatrix} i_m(t) \\ n_m(t) \end{bmatrix} + \begin{bmatrix} \frac{1}{L} \\ 0 \end{bmatrix} u(t), \\ \begin{bmatrix} y_1(t) \\ y_2(t) \end{bmatrix} &= \begin{bmatrix} 1 & 0 \\ 0 & 1 \end{bmatrix} \begin{bmatrix} x_1(t) \\ x_2(t) \end{bmatrix}, \end{aligned} \tag{55}$$

where $i_m$(A), $u$(V), $R(\Omega)$, $L$(H), $M_e$(V rad/s), $M_t$(N m/amp), $J_1$(J s$^2$/rad) and $f_r$(J s/rad) are current, armature voltage, resistance, inductance, back EMF constant, torque constant, motor inertia and friction coefficient, respectively. The parameters of the model are shown in Table 1.

**TABLE 1** Model parameters.

| **model**($i$) | $R$ | $L(10^{-3})$ | $M_e(10^{-2})$ | $J_1(10^{-4})$ | $f_r(10^{-4})$ |
|---|---|---|---|---|---|
| 0 | 1.2030 | 5.5840 | 8.1876 | 1.3528 | 2.3396 |
| 1 | 1.2030 | 8.7548 | 8.1876 | 1.3528 | 2.3396 |

The torque constant $M_t$ can be obtained from the back EMF constant $M_e$ as follows: $M_t = 1.0005 M_e$. In order to operate the motor at the speed to 70.3(rad/s), the control input $u_c = 6$ V is applied.

The Euler method is used to discretize (55). Considering the model uncertainties and after time discretization, the discrete-time linear model is obtained as follows

$$\begin{cases} x_{k+1} = A(\theta)x_k + Bu_k + B_\omega \omega_k, \\ y_k = Cx_k + D_\upsilon \upsilon_k, \end{cases} \tag{56}$$

where

$$A(\theta) \triangleq [A] = A + \Theta, \tag{57}$$

and $\Theta = \begin{bmatrix} \theta & 0 \\ 0 & \theta \end{bmatrix}$ is uncertain matrix, $|\theta| \leq 0.03$. When the system is in the model $i = 0$, the system is healthy operation

$$A^{[0]} = \begin{bmatrix} 0.286 & -0.043 \\ 1.771 & 0.914 \end{bmatrix},\ B^{[0]} = \begin{bmatrix} 0.529 & 0.953 \end{bmatrix},\ C^{[0]} = \begin{bmatrix} 1 & 0 \\ 0 & 1 \end{bmatrix},\ B_\omega^{[0]} = \begin{bmatrix} -0.0254 & -0.0778 \\ -0.3996 & 0.3026 \end{bmatrix},\ D_\upsilon^{[0]} = \begin{bmatrix} 1 & 0 \\ 0 & 1 \end{bmatrix}.$$

When a fault occurs, the parameter matrices of the system are

$$A^{[1]} = \begin{bmatrix} 0.459 & -0.033 \\ 2.121 & 0.936 \end{bmatrix},\ B^{[1]} = \begin{bmatrix} 0.404 & 0.684 \end{bmatrix},\ C^{[1]} = \begin{bmatrix} 1 & 0 \\ 0 & 1 \end{bmatrix},\ B_\omega^{[1]} = \begin{bmatrix} -0.0254 & -0.0778 \\ -0.3996 & 0.3026 \end{bmatrix},\ D_\upsilon^{[1]} = \begin{bmatrix} 1 & 0 \\ 0 & 1 \end{bmatrix}.$$

The simulation results presented in the following are obtained considering that the initial state, measurement noise, and process disturbance of the system satisfy the following bounds

$$\begin{aligned} \boldsymbol{x}_0 &\in \mathcal{X}_0 = \left\langle \begin{bmatrix} 0.6 \\ 70 \end{bmatrix} \begin{bmatrix} 0.06 & 0 \\ 0 & 0.6 \end{bmatrix} \right\rangle, \\ \boldsymbol{\upsilon}_k &\in \mathcal{V} = \left\langle \begin{bmatrix} 0 \\ 0 \end{bmatrix} \begin{bmatrix} 0.06 & 0 \\ 0 & 0.6 \end{bmatrix} \right\rangle, \\ \boldsymbol{w}_k &\in \mathcal{W} = \langle \mathbf{0}, I_2 \rangle. \end{aligned} \tag{58}$$

Assume that the actual system is operating as follows

$$\text{system} = \begin{cases} \text{healthy} & 0 \leq k < 20, \\ \text{faulty} & 20 \leq k < 40, \\ \text{healthy} & 40 \leq k < 60. \end{cases} \tag{59}$$

Figure 3 shows the output sets of healthy and faulty in case that auxiliary input signal is not used. In this figure, the red zonotopes and the blue zonotope are the output sets of the healthy and the faulty models, respectively. Black circles represent the output of actual system. When the auxiliary input signal is not injected into the system, the output set of the healthy model intersects with the output set of the faulty model. When the actual system belongs to the intersecting part, it is impossible to

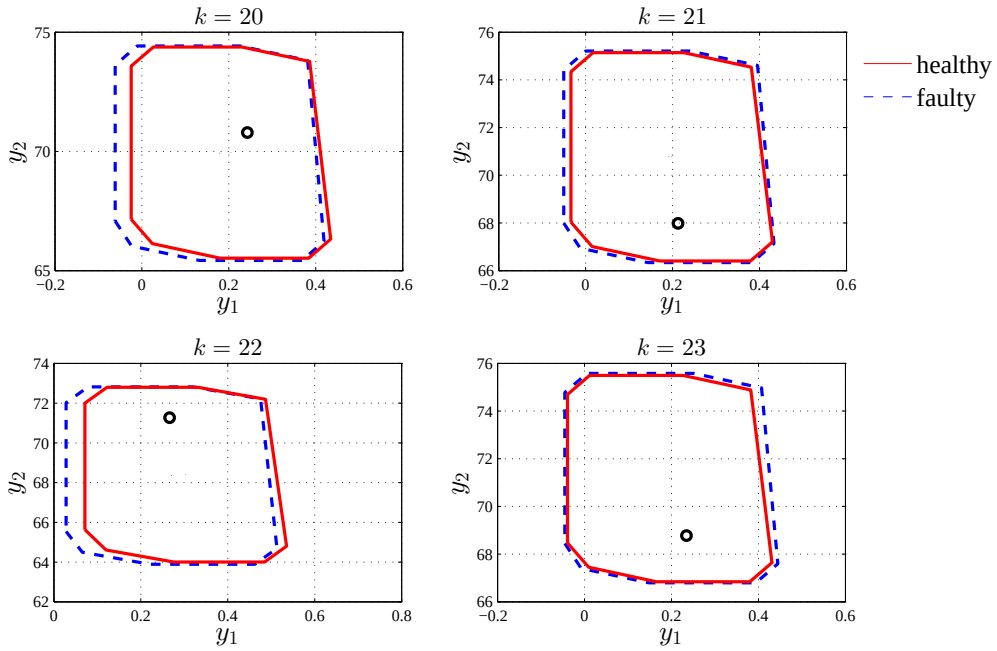


**FIGURE 3** The output sets of healthy and faulty without auxiliary input signal.

detect whether the fault has occurred. Therefore, in order to detect faults in the system, a proper auxiliary input signal is needed to separate the healthy output sets from the faulty output sets.

In order to verify the effectiveness of the proposed method, the additional methods are used for comparison.

- Method ①: Considering system parameter uncertainties, auxiliary input signal is generated based on output zonotopes without observers.

  For system (10), it is assumed that the state at sample time $k$ is $\tilde{x}_k^{[i]} \in \tilde{\mathcal{X}}_k^{[i]} = \langle \tilde{p}_k^{[i]}, \tilde{H}_k^{[i]} \rangle$. The state at sample time $k+1$ is

$$\tilde{x}_{k+1}^{[i]} \in \tilde{\mathcal{X}}_{k+1}^{[i]} = \langle \tilde{p}_{k+1}^{[i]}, \tilde{H}_{k+1}^{[i]} \rangle, \tag{60}$$

  where

$$\begin{cases} \tilde{p}_{k+1}^{[i]} = \mathrm{mid}([A^{[i]}])\tilde{p}_k^{[i]} + B^{[i]}u_k, \\ \tilde{H}_{k+1}^{[i]} = \left[\mathrm{mid}([A^{[i]}])\tilde{H}_k^{[i]} \;\; \mathrm{rs}(\mathrm{rad}([A^{[i]}]))\left|\tilde{H}_k^{[i]}\right| \;\; \mathrm{rs}(\mathrm{rad}([A^{[i]}]))\left|\tilde{p}_k^{[i]}\right| \;\; B_\omega^{[i]} H_\omega^{[i]}\right]. \end{cases} \tag{61}$$

  Therefore, the zonotope of output system is

$$\tilde{y}_{k+1}^{[i]} \in \tilde{\mathcal{Y}}_{y,k+1}^{[i]} = \left\langle \tilde{p}_{y,k+1}^{[i]}, \tilde{H}_{y,k+1}^{[i]} \right\rangle, \tag{62}$$

  where

$$\begin{cases} \tilde{p}_{y,k+1}^{[i]} = C^{[i]}\tilde{p}_k^{[i]}, \\ \tilde{H}_{y,k+1}^{[i]} = \left[C^{[i]}\tilde{H}_{k+1}^{[i]} \;\; D_v^{[i]} H_v^{[i]}\right]. \end{cases} \tag{63}$$

- Method ②: Observer-based fault detection method without considering system parameter uncertainties.

  Assuming that the state at sample time $k$ is $\tilde{\tilde{x}}_k^{[i]} \in \tilde{\tilde{\mathcal{X}}}_k^{[i]} = \left\langle \tilde{\tilde{p}}_k^{[i]}, \tilde{\tilde{H}}_k^{[i]} \right\rangle$. The state at sample time $k+1$ is

$$\tilde{\tilde{x}}_{k+1}^{[i]} \in \tilde{\tilde{\mathcal{X}}}_{k+1}^{[i]} = \left\langle \tilde{\tilde{p}}_{k+1}^{[i]}, \tilde{\tilde{H}}_{k+1}^{[i]} \right\rangle, \tag{64}$$

where

$$\begin{cases} \tilde{\tilde{p}}_{k+1}^{[i]} = A^{[i]}\tilde{\tilde{p}}_{k}^{[i]} + B^{[i]}u_k, \\ \tilde{\tilde{H}}_{k+1}^{[i]} = \left[A^{[i]}\tilde{\tilde{H}}_{k}^{[i]} \;\; B_{\omega}^{[i]}H_{\omega}^{[i]}\right]. \end{cases} \tag{65}$$

Therefore, the zonotope of output system can be written as

$$\tilde{\tilde{y}}_{k+1}^{[i]} \in \tilde{\tilde{\mathcal{Y}}}_{y,k+1}^{[i]} = \left\langle \tilde{\tilde{p}}_{y,k+1}^{[i]}, \tilde{\tilde{H}}_{y,k+1}^{[i]} \right\rangle, \tag{66}$$

where

$$\begin{cases} \tilde{\tilde{p}}_{y,k+1}^{[i]} = C^{[i]}\tilde{\tilde{p}}_{k}^{[i]}, \\ \tilde{\tilde{H}}_{y,k+1}^{[i]} = \left[C^{[i]}\tilde{\tilde{H}}_{k+1}^{[i]} \;\; D_{v}^{[i]}H_{v}^{[i]}\right]. \end{cases} \tag{67}$$

Figures 4−6 show the size of the generated input signals, the influence of the auxiliary input signal on system and the size of the output zonotope with the method ①, method ② and the proposed method, respectively. In Figure 4, the purple dashed line, blue dotted line and red solid line are the auxiliary input signals obtained by method ①, method ② and the proposed method, respectively. The amplitudes of auxiliary input signals by method ② and the proposed method are smaller than method ①. Also, it can be seen that the influence of the input signals based on Method ① is largest then the other two. The size of the output zonotope can be obtained by means of Property 6. According to the idea of active FD, the larger the volume of the output zonotopes, the greater volume of the intersection of the output zonotopes, so a larger auxiliary input signal is required to separate them. In Figure 6, $V_1$ and $V_2$ represent the size of the output zonotopes in healthy and faulty models, respectively.

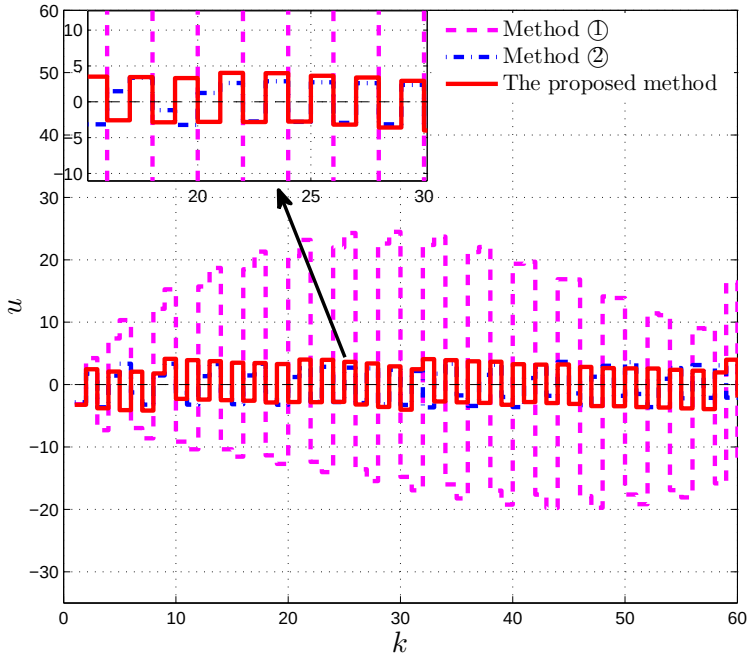


**FIGURE 4** The auxiliary input signal.

Figure 7 and Figure 8 show the output sets for the healthy and faulty models after the auxiliary input signal designed with the method proposed is injected into the system from $k = 20$ until $k = 23$ and from $k = 40$ until $k = 43$, respectively. In these figures, the red zonotopes are the output sets of the healthy model, and the blue zonotope are the output sets of faulty model, respectively. Black circles represent the output of the actual system. In Figure 7, the actual system output falls in the output zonotope of the faulty model at $k = 21$. This means that the fault is detected since $k = 21$, because at $k = 20$ the actual output was still in output zonotope of the healthy model. According to (59), the system present the fault from $k = 20$, so there is time

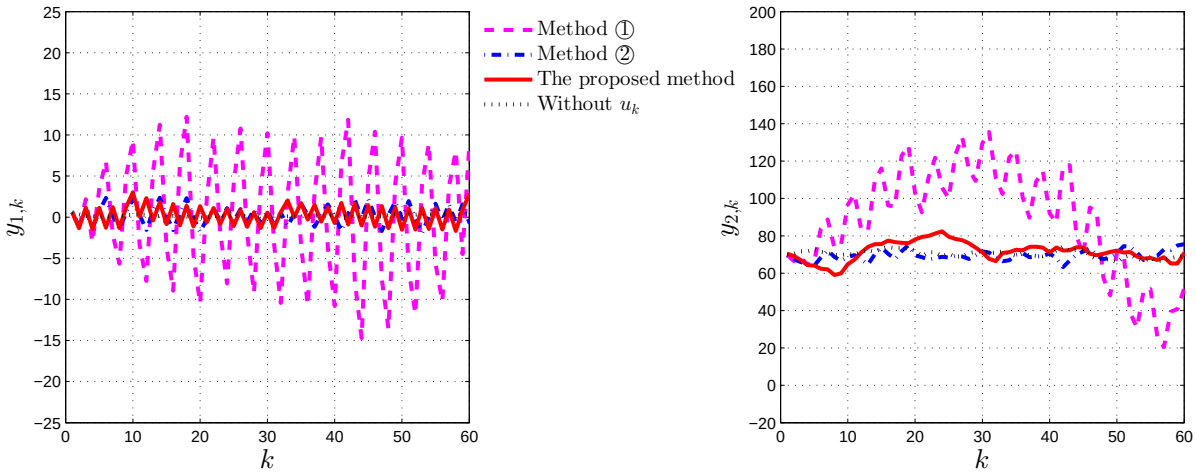


**FIGURE 5** The effect of auxiliary input signal on system output.

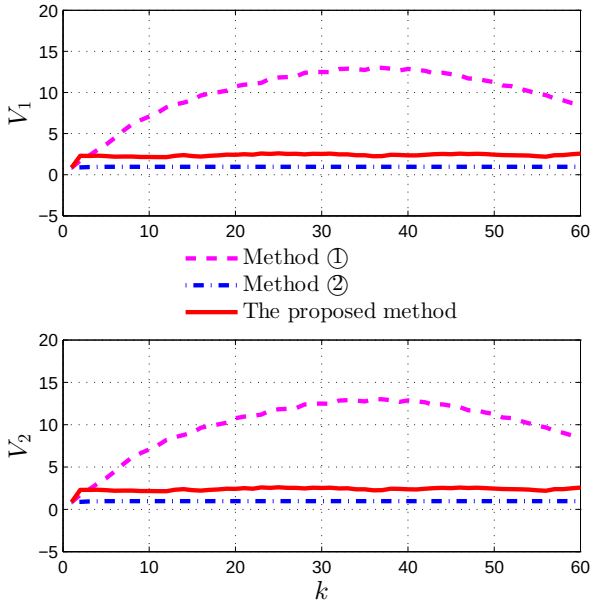


**FIGURE 6** The size of zonotope.

delay of one sample time in the fault detection process. Similarly, the output of actual system falls in the output zonotope of the healthy model at $k = 41$, so the system is detected to be in the faulty state at this time.

The comparison of the fault detection results between the proposed method and methods ① and ② are presented in Figure 9. These result are obtained by checking the conditions (53) with the method proposed in Remark 2. Since method ② doesn't consider the system parameter uncertainties, it may generate some wrong fault detection results.

According to Figure 4 and Figure 9, the auxiliary input signal obtained by the method ② is the smallest, but the detectability of faults is poor. Method ① presents satisfactory detection results, but the auxiliary input signal is big (see Figure 4). Compared to the other two methods, the proposed method has a small auxiliary input signal and can correctly detect the system model. In summary, the proposed method has advantages because of the smaller auxiliary input signals required while presenting satisfactory detection results.

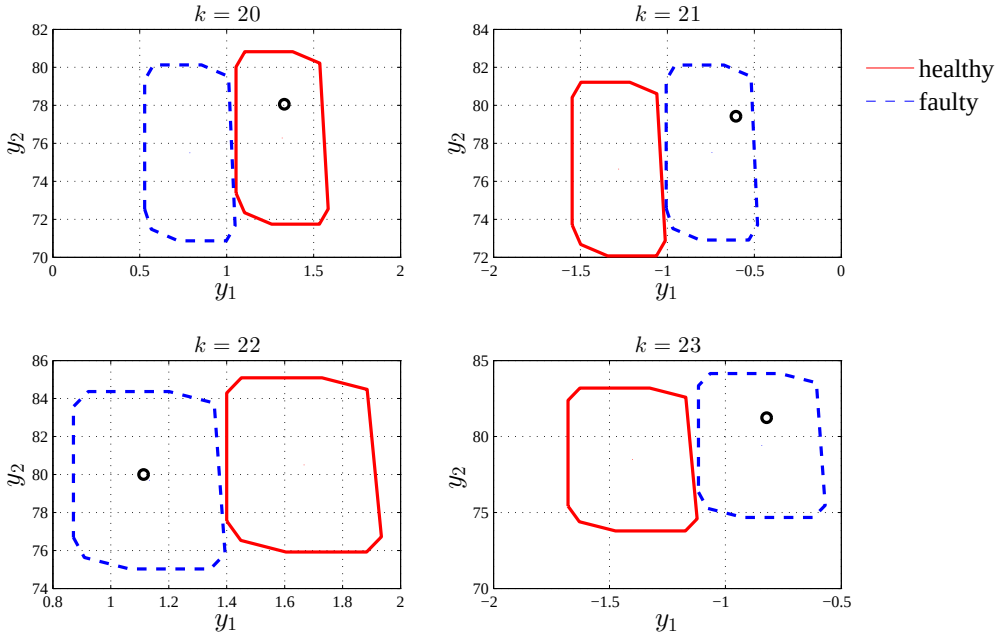


**FIGURE 7** The output sets of healthy and faulty obtained by the proposed method model.

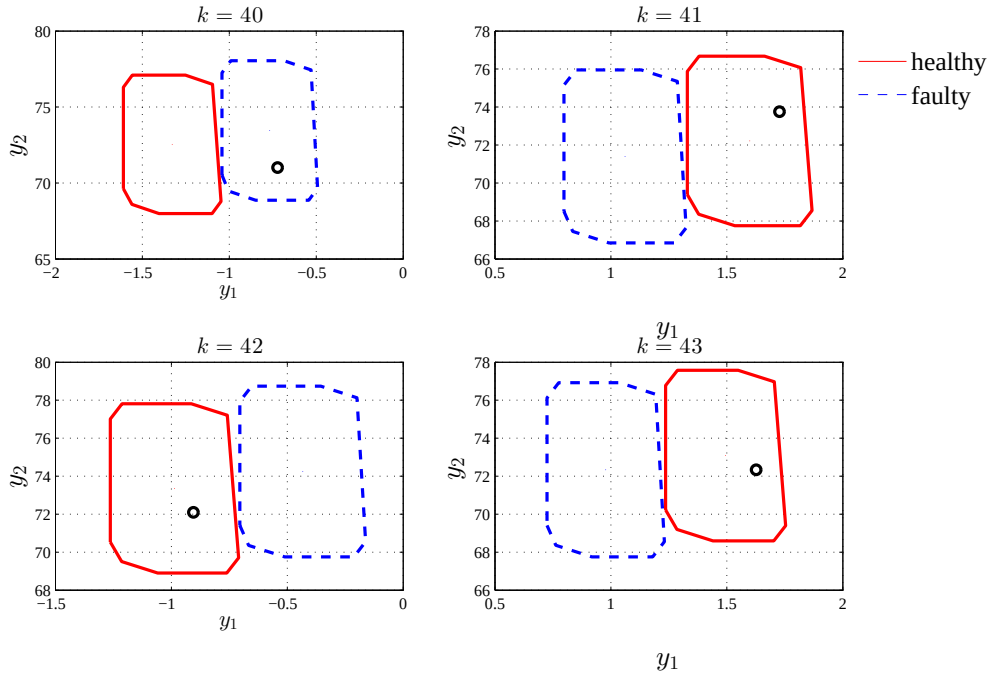


**FIGURE 8** The output sets of healthy and faulty model obtained by the proposed method.

## 6 | CONCLUSIONS

In this paper, an active FD method based on set-membership approach for uncertain discrete-time system is proposed. Firstly, a zonotopic observer is designed with the aim of minimizing the set that bounds the output estimated set. This is achieved by

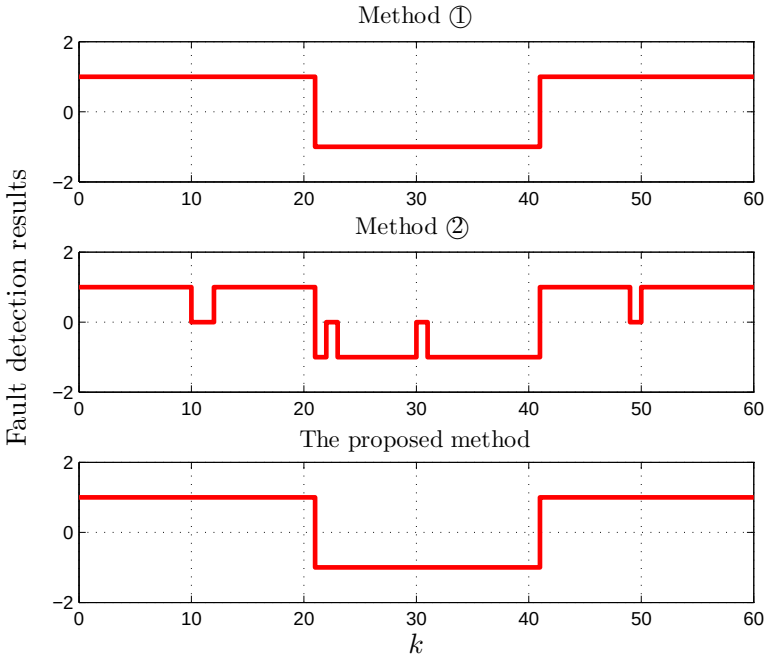


**FIGURE 9** The result of fault detection.

means of a time-varying gain of the observer that is obtained by minimizing the size of the zonotope bounding output sets. Then, a proper auxiliary input signal is designed to separate the output zonotopes of the healthy model from the output zonotopes of the faulty model. Finally, the input signal is injected into the system to detect small faults. Based on the results obtained using the considered case study, the proposed method reduces the size of the output zonotopes and conservativeness of the auxiliary input signal design process by using zonotpic observers. Since the auxiliary input signal belongs to an external signal, the addition of the auxiliary input signal will have an impact on the system. Therefore, a method for further reducing the conservativeness will be focused on in future research.

## ACKNOWLEDGMENTS

J. Wang is thankful for the grant funded by NSFC (61973023, 61573050) and the Fundamental Research Funds for the Central Universities (No. XK1802-4).
M. Zhou is thankful for the grant funded by NSFC (51805021) and China Postdoctoral Science Foundation Grant (No. 2018M631311).

## References

1. Xu F, Tan J, Wang X, et al. Generalized set-theoretic unknown input observer for LPV systems with application to state estimation and robust fault detection. *Int J Robust Nonlinear Control.* 2017; 27: 3812 – 3832.

2. Wang Y, Puig V, Cembrano G. Robust fault estimation based on zonotopic Kalman filter for discrete-time descriptor systems. *Int J Robust Nonlinear Control.* 2018; 28(16): 5071 – 5086.

3. Li X, Zhu F. Fault-tolerant control for Markovian jump systems with general uncertain transition rates against simultaneous actuator and sensor faults. *Int J Robust Nonlinear Control.* 2017; 27(18): 4245 – 4274.

4. Nikoukhah R, Campbell S, Drake K. An active approach for detection of incipient faults. *Int J Syst Sci.* 2010; 41: 241 – 257.

5. Pourasghar M, Puig V, Ocampo-Martinez C. Interval observer versus set-membership approaches for fault detection in uncertain systems using zonotopes. *Int J Robust Nonlinear Control.* 2019; 29: 2819 – 2843.

6. Zhou M, Wang Z, Shen Y, Shen M. H_/H∞ fault detection observer design in finite-frequency domain for Lipschitz nonlinear systems. *IET Control Theory Appl.* 2017; 11(14): 2361 – 2369.

7. Zhang Q, Geng S. Dynamic uncertain causality graph applied to dynamic fault diagnoses of large and complex systems. *IEEE Trans Reliability.* 2015; 64(3): 910 – 927.

8. Kallas M, Mourot G, Maquin D, Ragot J. Data-driven approach for fault detection and isolation in nonlinear system. *Int J Robust Nonlinear Control.* 2018; 32: 1569 – 1590.

9. Cai B, Zhao Y, Liu H, Xie M. A data-driven fault diagnosis methodology in three-phase inverters for PMSM drive systems. *IEEE Trans Power Electronics.* 2017; 32(7): 5590 – 5600.

10. Šimandl M J, Punčochář I. Active fault detection and control: Unified formulation and optimal design. *Automatica.* 2009; 45: 2052 – 2059.

11. Punčochář I, Škach J. A survey of active fault diagnosis methods. *IFAC-PapersOnline.* 2018; 51(24): 1091 – 1098.

12. Wang J, Zhang J, Qu B, Wu H, Zhou J. Unified architecture of active fault detection and partial active fault-tolerant control for incipient faults. *IEEE Trans Syst Man Cybernetics Syst.* 2017; 47(7): 1688 – 1700.

13. Marseglia G, Raimondo D. Active fault diagnosis: A multi-parametric approach. *Automatica.* 2017; 79: 223 – 230.

14. Kerestecioğlu F, Çetin I. Optimal input design for the detection of changes towards unknown hypotheses. *Int J Syst Sci.* 2004; 35(7): 435 – 444.

15. Škach J, Punčochář I, Lewis F. Optimal active fault diagnosis by temporal-difference learning. In: Proceedings of IEEE 55th Conference on Decision and Control. ; December 12 – 14, 2016; Las Vegas, USA.

16. Garulli A, Vicino A. Set membership localization of mobile robots via angle measurements. *IEEE Trans Robot Autom.* 2001; 17(4): 450 – 463.

17. Zhai S, Wang W, Ye H. Auxiliary signal design for active fault detection based on set-membership. *IFAC-PapersOnLine.* 2015; 48(21): 452 – 457.

18. Wang J, Wang J, Zhou J. On-line active fault detection based on set-membership ellipsoid and moving window. In: Proceedings of IEEE 7th Data Driven Control and Learning Systems Conference. ; 2018: 420 – 425.

19. Scott J, Findeisen R, Braatz R, Raimondo D. Design of active inputs for set-based fault diagnosis. In: Proceedings of American Control Conference. ; 2013; Washington, DC, USA.

20. Raimondo D, Marseglia G, Braatz D, Scott J. Closed-loop input design for guaranteed fault diagnosis using set-valued observers. *Automatica.* 2016; 74: 107 – 117.

21. Tabatabaeipour S. Active fault detection and isolation of linear time varying systems: a set-membership approach. *Int J Syst Sci.* 2013: 1917 – 1933.

22. Campbell S, Horton K, Nikoukhah R. Auxiliary signal design for rapid multi-model identification using optimization. *Automatica.* 2002; 38: 1313 – 1325.

23. Campbell S, R N. *Auxiliary signal design for failure detection*. Princeton University Press . 2004.

24. Zhou M, Cao Z, Zhou M, Wang J, Wang Z. Zonotoptic fault estimation for discrete-time LPV systems with bounded parametric uncertainty. *IEEE Trans Intell Transp Syst.* 2019. doi: 10.1109/TITS.2019.2898853.

25. Combastel C. Merging Kalman filtering and zonotopic state bounding for robust fault detection under noisy environment. *IFAC – PapersOnLine.* 2015; 48(21): 289 – 295.

26. Alamo T, Bravo J, Camacho E. Guaranteed state estimation by zonotopes. *Automatica.* 2005; 41(6): 1035 – 1043.

27. Le V, Stoica C, Alamo T, Camacho E, Dumur D. Zonotopic guaranteed state estimation for uncertain systems. *Automatica.* 2013; 49: 3418 – 3424.

28. Wang Y, Puig V, Cembrano G. Set-membership approach and Kalman observer based on zonotopes for discrete-time descriptor systems. *Automatica.* 2018; 93: 435 – 443.

29. Combastel C. A state bounding observer for uncertain non-linear continuous-time systems based on zonotopes. In: Proceedings of the 44th IEEE Conference on Decision and Control. ; December 12 – 15, 2005; Seville, Spain: 7228 – 7234.

30. Scott J, Findeisen R, Braatz R, Raimondo D. Input design for guaranteed fault diagnosis using zonotopes. *Automatica.* 2014; 50(6): 1580 – 1589.

31. Dobkin D, Hershberger J, Kirkpatrick D, Suri S. Computing the intersection-depth of polyhedra. *Algorithmica.* 1998; 9: 518 – 533.

32. Pourasghar M, Puig V, Ocampo-Martinez C. Characterisation of interval-observer fault detection and isolation properties using the set-invariance approach. *Journal of the Franklin Institute.* 2019.

33. Wang Y, Wang Z, Puig V, Cembrano G. Zonotopic set-membership state estimation for discrete-Time descriptor LPV systems. *IEEE Trans Autom Control.* 2019; 64(5): 2092 – 2099.

34. Combastel C. Zonotopes and Kalman observers: Gain optimality under distinct uncertainty paradigms and robust convergence. *Automatica.* 2015; 55: 265 – 273.

35. Bertsekas D. *Nonlinear programming*. Belmont, MA: Athena Scientific . 1999.

36. Zhang J, Yuan C, Stegagno P, zang W, Wang C. Small fault detection from discrete-time closed-loop control using fault dynamics residuals. *Neurocomputing.* 2019; 365: 239 – 248.

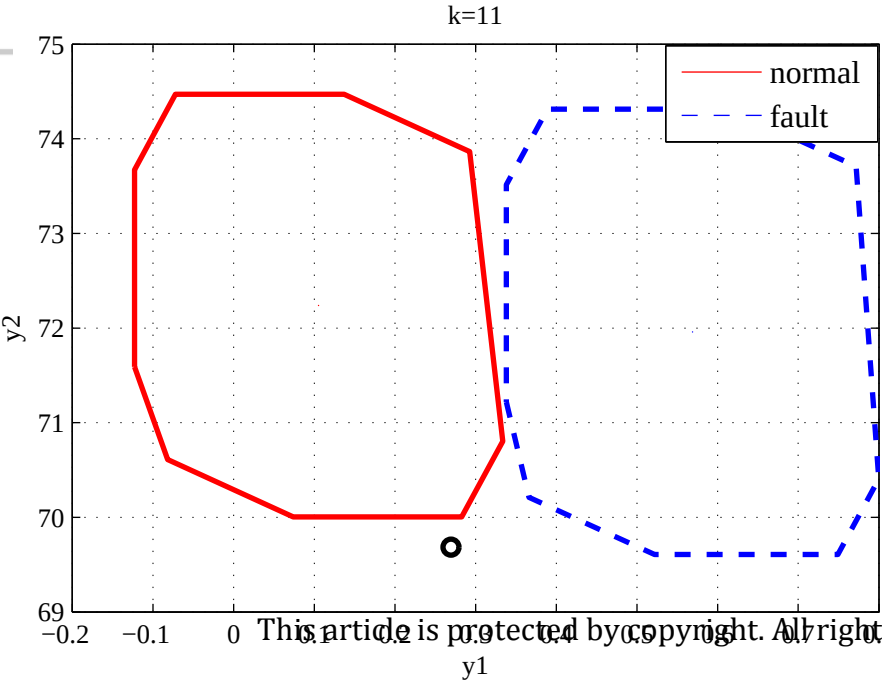

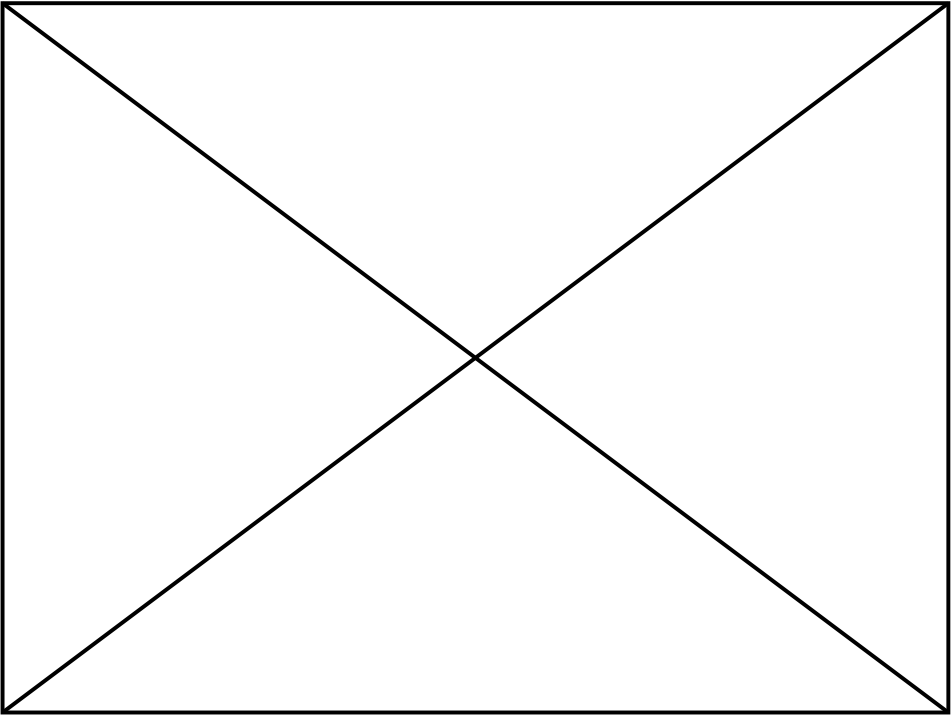

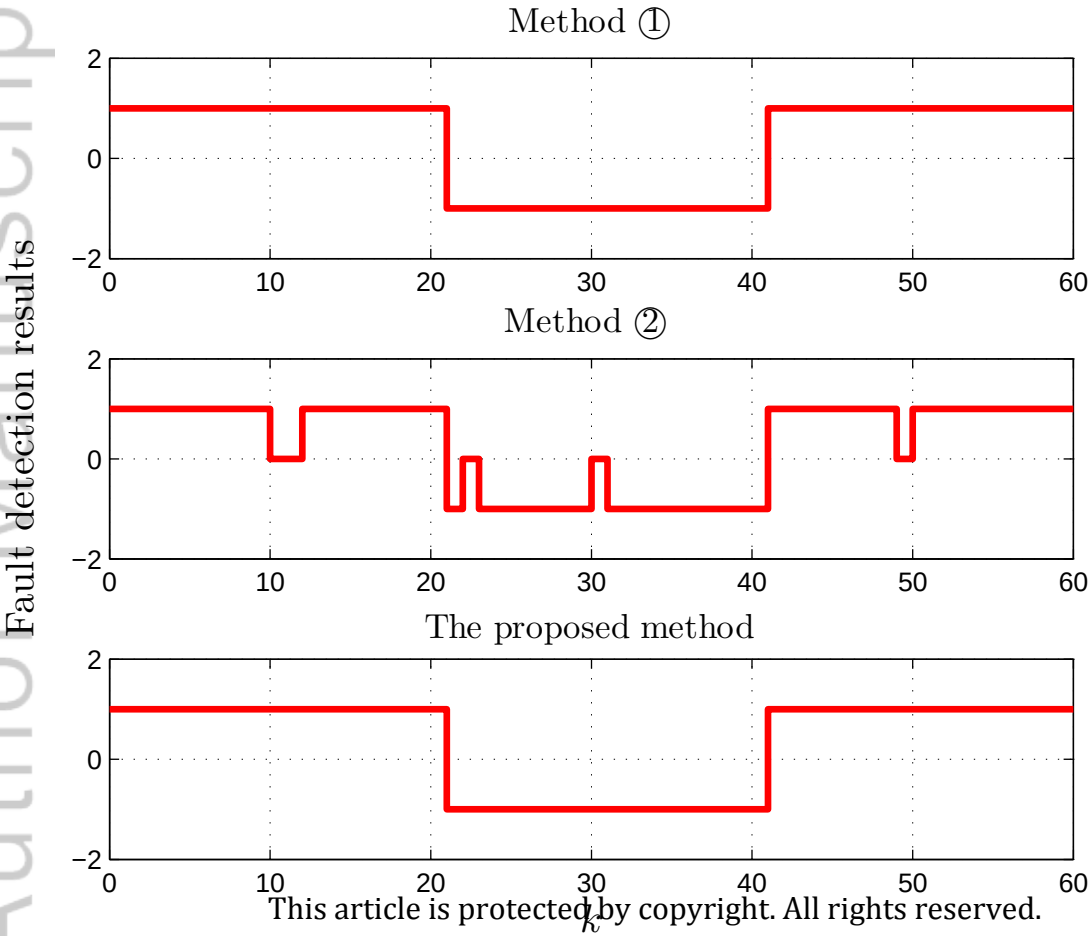

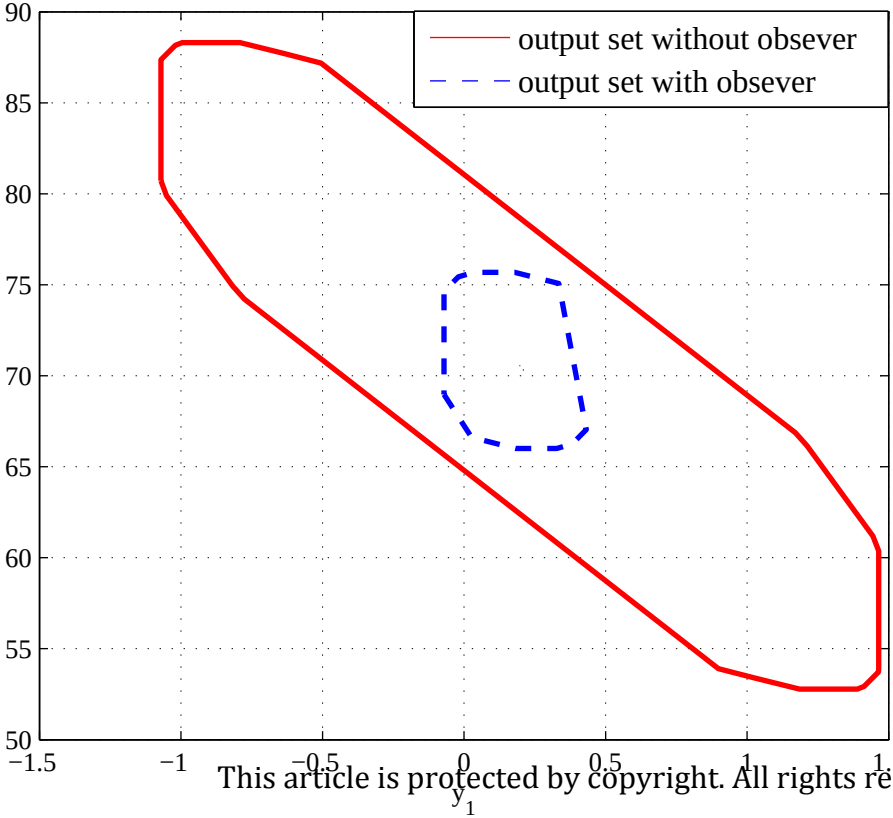

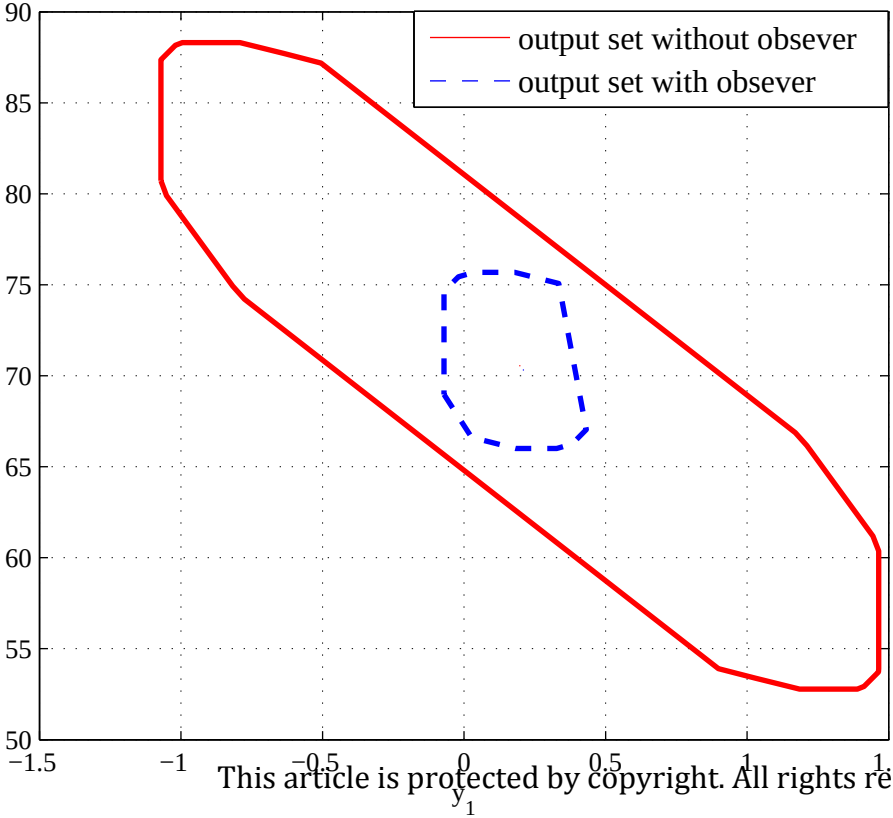

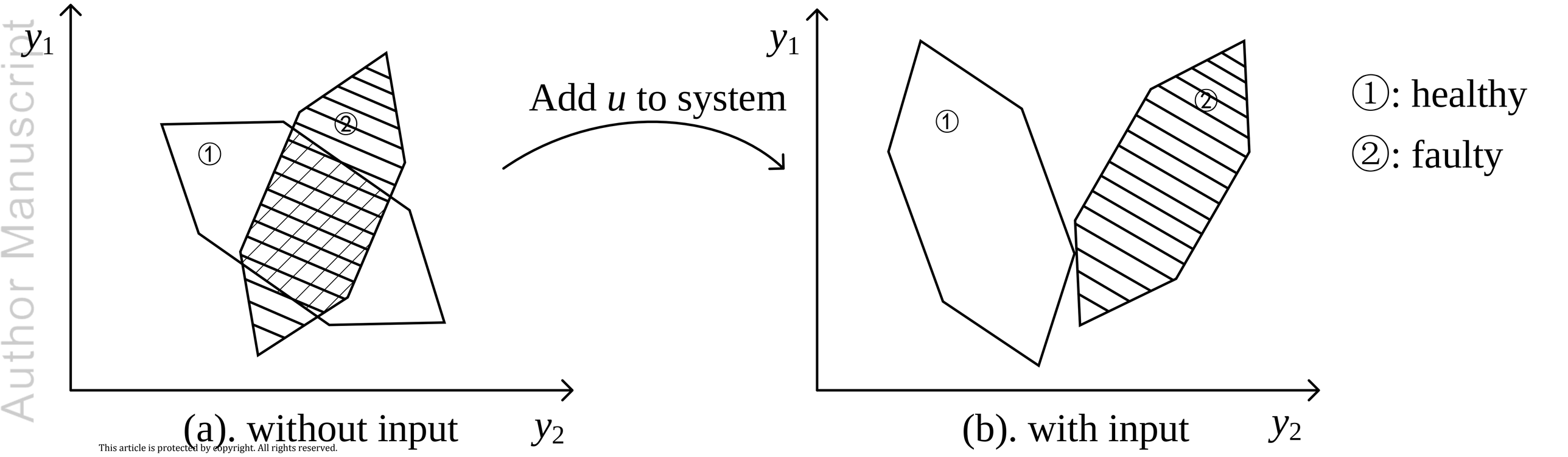

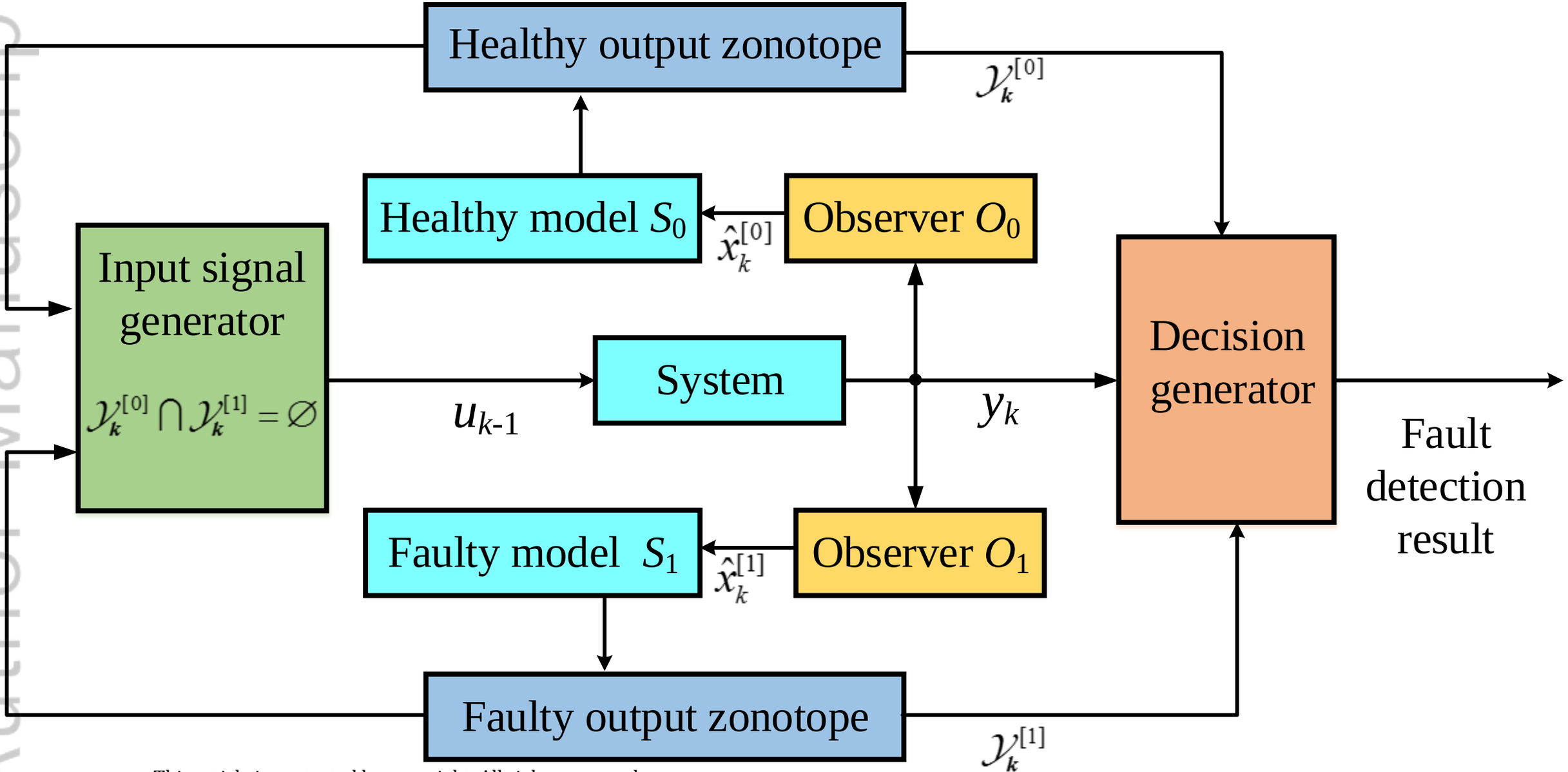

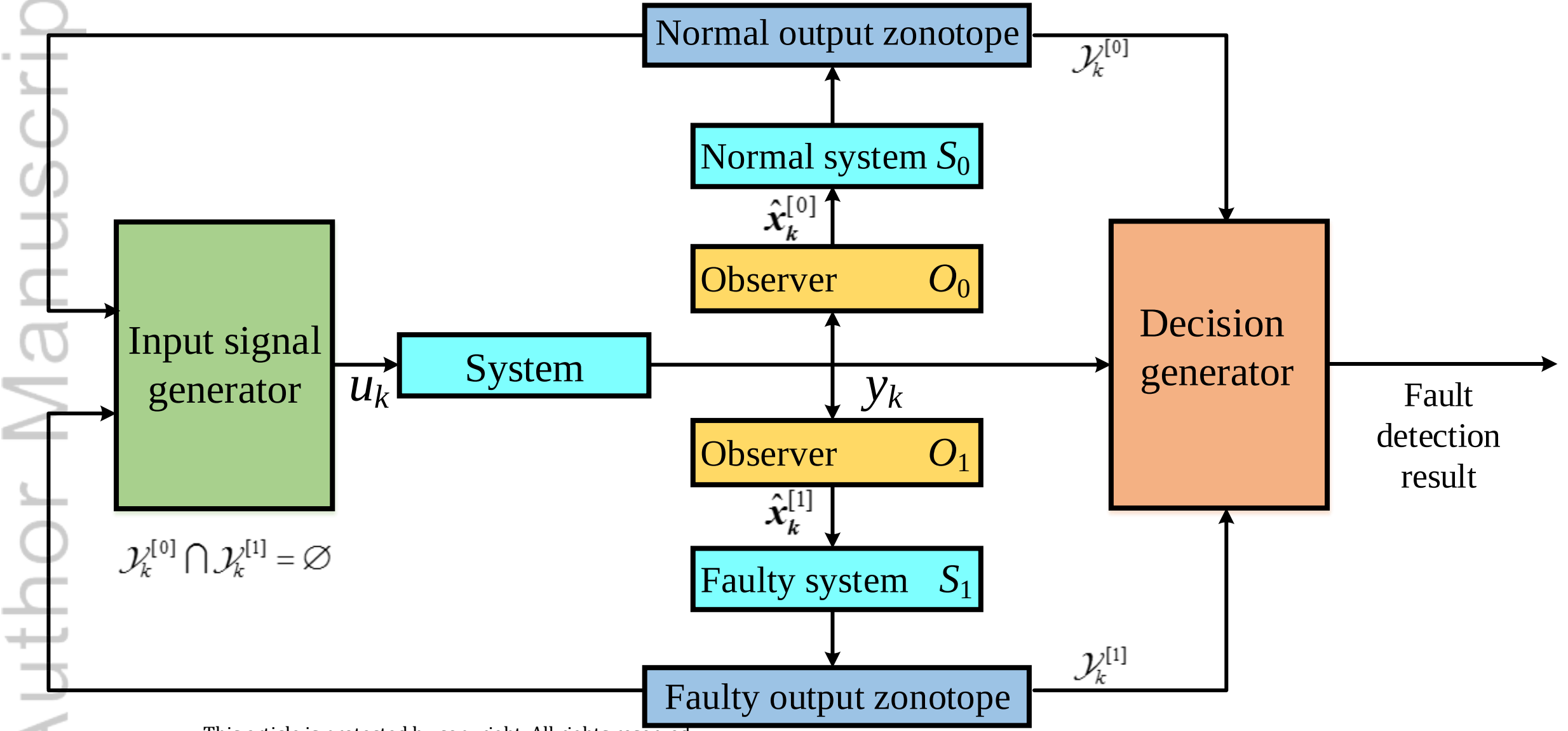

Received: Added at production | Revised: Added at production | Accepted: Added at production

DOI: xxx/xxxx

ARTICLE TYPE

# Active fault detection based on set-membership approach for uncertain discrete-time systems

Jing Wang[1,2] | Yuru Shi[2] | Meng Zhou*[1] | Ye Wang[3] | Vicenç Puig[4]

[1]School of Electrical and Control Engineering, North China University of Technology, Beijing, China
[2]College of Information Science and Technology, Beijing University of Chemical Technology, Beijing, China
[3]College of Automation, Harbin Engineering University, Harbin, China
[4]Advanced Control Systems Research Group at Institutde Robòtical, CSIC-UPC, Universitat Politècnica de Catalunya-BarcelonaTech, Barcelone, Spain

**Correspondence**
*Meng Zhou, School of Electrical and Control Engineering, North China University of Technology, Beijing,100144, China. Email: zhoumeng@mail.buct.edu.cn

**Summary**

Active fault detection facilitates the determination of the fault characteristics by injecting proper auxiliary input signals into the system. This paper proposes an observer-based on-line active fault detection method for discrete-time systems with bounded uncertainties. First, the output including disturbances, measurement noise and interval uncertainties at each sample time is enclosed into a zonotope. In order to reduce the conservativeness in the fault detection process, a zonotopic observer is designed to estimate the system states allowing to generate the output zonotopes. Then, a proper auxiliary input signal is designed to separate the output zonotopes of the faulty model from the healthy model that is injected into the system to facilitate the fault detection. Since the auxiliary input signal generation leads to a non-convex optimization problem, it is transformed into a mixed integer quadratic programming problem. Finally, a case study based on a DC motor is used to show the effectiveness of the proposed method.

**KEYWORDS:**
active fault detection, small fault, interval uncertainty, zonotope, set-membership

## 1 | INTRODUCTION

In modern industries, operational safety and product quality of systems are important issues. If a fault occurs, it will not only affect the quality of the product, but it can also consequently bring security risks to the systems and operators. Therefore, fault diagnosis (FD)[1,2] plays a crucial role in industrial processes. Over the past decades, an important number of FD methods have been developed. These methods can be classified into passive[3] and active FD[4] depending if the system input is manipulated or not. In passive FD, the system is monitored using the system inputs and outputs without manipulation. Passive FD approaches can be divided into model-based methods[5,6], knowledge-based methods[7], and data-driven methods[8,9]. On the other hand, the key idea of active FD is to enhance the output separability of the healthy model from the faulty ones by manipulating the input signal[10]. In this way, the fault characteristics become more clear allowing that smaller faults can be detected. For this reason, active FD has attracted increasing researcher attention in recent years. Active FD methods mainly include deterministic and probabilistic methods depending on the underlying assumptions regarding system noise and disturbance[11]. The deterministic methods assume that the noise and disturbances can be modeled as an unknown but bounded signal. Examples of such methods are the integrated controller and detector design method and the guaranteed fault diagnosis approach[12,13]. Probabilistic methods assume that uncertainties such as noise and disturbance affecting the system can be represented by random variables with known probability density functions. Then, fault detection is based on probabilistic methods such as statistical tests[14] or the Bayesian approach[15].

Most of the existing active FD methods assume that the noise and system disturbance follow a Gaussian distribution. However, such a prior knowledge of the probability distribution of the noise and disturbance in the actual system is difficult to be satisfied in practice [16]. On the other hand, the active set-membership methods FD generally do not assume any prior information regarding measurement noise and process disturbance distribution of the system except that they are unknown but the upper and lower bounds are known. The set-membership approaches allow to establish the separability conditions between faulty and non-faulty case in a guaranteed way by using the bounded description of the uncertainty and noises/disturbances. These conditions are then used to design an auxiliary input signal guaranteeing the separability of the healthy from the faulty modes improving FD performance. Therefore, compared with other active fault detection methods, the set-membership approach provides a framework for active fault detection with separability guarantees. Set-membership approaches compute a set containing all the possible system outputs/states that are consistent with the unknown but bounded disturbances, modeling uncertainties and measurement noise. Hence, it is a suitable technique for state estimation when a system is modeled by some unknown but bounded disturbances. Several alternative set descriptions have been considered in the literature including ellipsoids, intervals, polytopes and zonotopes [17].

In the field of guaranteed active FD, elliposidal sets have been widely used for bounding uncertainty. Then, active FD is realized by designing auxiliary input signals off-line [18] or on-line [19]. Compared with ellipsoids, zonotopes produces less conservative results when designing auxiliary input signals. Moreover, they can be used not only in the design of auxiliary input signals for open-loop systems [20], but also for closed-loop systems [21]. In addition, the idea of active FD based on set-membership approach is also used for active fault isolation [22] and multi-model separation [23].

Generally, the existing active FD methods based on the set-membership approach mainly use the idea of the set theory to bound system outputs using sets and the model [24]. The use of observers can not only used to reduce the size of the system output sets but to guarantee the convergence of the estimations. Therefore, in this paper, the zonotopic Kalman filter method is used, which reduces the size of the estimated system output sets. It should be mentioned that the uncertain system contains not only process disturbance and measurement noise, but also the uncertainties of system parameters, increasing the size of the minimum detectable faults. To the best knowledge of the authors', little attention has been paid on active fault detection based on set-membership method for system with parametric uncertainty. In the work of Zhou [25], an interval fault estimation approach is proposed for discrete-time linear parameter-varying systems, however, it deals with the problem of passive fault detection. Motivated by the work [25], in our work, we mainly focused on designing a proper auxiliary input signal for discrete-time system with parametric uncertainties to reduce the size of the minimum detectable faults.

The main contributions of this paper can be summarized as follows: First, an active fault detection method is proposed based on zonotopic Kalman filter observer for discrete-time system with bounded uncertainties. Following the earlier work regarding active fault detection based on the set-membership approach, we first apply this method to discrete-time system with parametric uncertainty, in which an auxiliary input signal is designed to separate the output zonotopes in the healthy case from the output zonotopes in the faulty case. Besides, in order to reduce the conservatism of auxiliary input signal design process, a zonotopic observer is designed to estimate the system output zonotope. Finally, the proposed approach is assessed using a case study based on a DC motor showing an improved detection in case of small faults.

The remainder of the paper is organized as follows. First, in Section 2, some preliminaries and the statement of the problem formulation used in this paper are introduced. Then, the zonotopic observer is designed to reduce the output set size in Section 3. An optimal auxiliary input signal is obtained by using output sets in Section 4. In Section 5, a DC motor is used as a case study and the simulation results show the effectiveness of the proposed method. Finally, the conclusion of this paper is introduced in Section 6.

## 2 | PRELIMINARIES AND PROBLEM FORMULATION

### 2.1 | Preliminaries

**Definition 1.** The $r$ order zonotope $\mathcal{Z}$ is defined as

$$\mathcal{Z} = p + \sum_{j=1}^{r} \alpha_j h_j = p \oplus H\mathbf{B}^r = \langle p, H \rangle, \tag{1}$$

where $p \in \mathbb{R}^n$ and $H = \{h_1, h_2, \cdots, h_r\} \in \mathbb{R}^{n\times r}$ are the center and the generator matrix of $\mathcal{Z}$, respectively. $\mathbf{B}^r = [-1, +1]^r$ is a unitary hypercube and $\|\alpha\|_\infty \leq 1$.

**Property 1.** Considering an interval $[a_1, a_2]$, $\text{mid}[a_1, a_2] = \frac{a_1+a_2}{2}$ and $\text{rad}[a_1, a_2] = \frac{a_2-a_1}{2}$ are the center and radius of the interval, respectively.

**Property 2.** Given an interval matrix $[A]$, where$A_{tj} = \{a_{tj} : a_{1,tj} \le a_{tj} \le a_{2,tj}\}$. The center and radius of the interval matrix are $\text{mid}[A]_{tj} = \frac{a_{1,tj}+a_{2,tj}}{2}$ and $\text{rad}[A]_{tj} = \frac{a_{2,tj}-a_{1,tj}}{2}$, respectively.

**Property 3.** The Minkowski sum of two zonotopes $\mathcal{Z}_1 = p_1 \oplus H_1\mathbf{B}^{r_1}$ and $\mathcal{Z}_2 = p_2 \oplus H_2\mathbf{B}^{r_2}$ is defined as

$$\mathcal{Z}_1 \oplus \mathcal{Z}_2 = \langle p_1, H_1\rangle \oplus \langle p_2, H_2\rangle = (p_1 + p_2) \oplus \begin{bmatrix} H_1 & H_2 \end{bmatrix} \mathbf{B}^{r_1+r_2}. \tag{2}$$

**Property 4.** The product of matrix $M$ and zonotope $\mathcal{Z} = \langle p, H\rangle$ is calculated as

$$M\mathcal{Z} = \langle Mp, MH\rangle . \tag{3}$$

**Property 5.** [26] Frobenius radius of the generator matrix $H$ can be used as an indicator to measure the size of the zonotope. It is expressed as

$$J = \sqrt{\text{tr}(H^T H)} = \sqrt{\text{tr}(HH^T)}\,, \tag{4}$$

where $\text{tr}(\cdot)$ is the matrix trace.

**Property 6.** [27] Considering a family of zonotopes represented by $\mathcal{Z} = p \oplus [H]\mathbb{B}^r$, where $p \in \mathbf{R}^n$ is a real vector, $[H] \in \mathbb{I}^{n\times r}$ is an interval matrix, $\mathbb{I}$ is defined as a set of real compact intervals. A family of zonotopes can be bounded by an outer approximation, as follows

$$\mathcal{Z} = p \oplus [\text{mid}[H]\ \ \text{rs}(\text{rad}[H])]\mathbf{B}^{r+n}\,. \tag{5}$$

where $\text{rs}(H) = \text{diag}(\sum_{j=1}^{r} \left|H_{n,j}\right|)$.

**Property 7.** [28] The product of an interval $[A]$ and a matrix $B$ denoted by $[A]B$ whose center and radius are $\text{mid}([A]\,B) = (\text{mid}\,[A])\,B$ and $\text{rad}\,([A]\,B) = (\text{rad}\,[A])\,|B|$, respectively. $|B|$ is the absolute value of each element in the matrix $B$.

**Lemma 1.** [29] A zonotope $\mathcal{Z}$ can be bounded by a minimal box $\square\mathcal{Z}$ known as interval hull

$$\mathcal{Z} \subset \square\mathcal{Z} = p \oplus \text{rs}(H)\mathbf{B}^r. \tag{6}$$

**Lemma 2.** [30] Let consider the $r$-order zonotope $\mathcal{Z} = p \oplus H\mathbf{B}^r \subset \mathbb{R}^n$ and the integer $n \le s \le r$. The column vector of the matrix $H$ is arranged in descending order of the Euclidean norm to obtain the matrix $\bar{H}$. $\mathcal{Z}$ can be included in a $s$-order $\bar{\mathcal{Z}}$, i.e.

$$\mathcal{Z} \subseteq \bar{\mathcal{Z}} = p \oplus \begin{bmatrix} \bar{H}_1 & Q \end{bmatrix} \mathbf{B}^s, \tag{7}$$

where $\bar{H}_1$ is the first $s - n$ column vectors of $\bar{H}$, $\bar{H}_2$ is the last $n$ column vectors of $\bar{H}$. $Q$ is the box containing $\bar{H}_2$ obtained by Lemma 1, i.e.

$$Q_{tt} = \sum_{j=1}^{r} \left|\bar{H}_2\right|_{tj}, t = 1, 2, \cdots, n. \tag{8}$$

**Lemma 3.** [31,32] Given two zonotopes $\mathcal{X} = \langle a_x + b_x, H_x\rangle$ and $\mathcal{Y} = \langle a_y + b_y, H_y\rangle$, $\mathcal{X} \bigcap \mathcal{Y} = \varnothing$ if and only if

$$a_y - a_x \notin \langle b_x, H_x\rangle \oplus \langle -b_y, H_y\rangle\,. \tag{9}$$

## 2.2 | Problem formulation

Let consider the class of uncertain discrete-time systems as:

$$\begin{cases} x_{k+1}^{[i]} = A^{[i]}(\theta)x_k^{[i]} + B^{[i]}u_k + B_\omega^{[i]}\omega_k^{[i]}, \\ y_k^{[i]} = C^{[i]}x_k^{[i]} + D_\upsilon^{[i]}\upsilon_k^{[i]}, \quad i = 0, 1, 2, \cdots, q, \end{cases} \tag{10}$$

where $i$ is the system model: the case $i = 0$ corresponds to the healthy model, otherwise, the other cases correspond to the faulty models, where $q$ denotes the total number of models. $x_k \in \mathbb{R}^{n_x}$, $u_k \in \mathbb{R}^{n_u}$,$y_k \in \mathbb{R}^{n_y}$ are state, input and output of the system at sample time $k$, respectively. $\omega_k \in \mathbb{R}^{n_\omega}$ and $\upsilon_k \in \mathbb{R}^{n_\upsilon}$ represent the process disturbance and measurement noise of the system, respectively. $A^{[i]}(\theta)$, $B^{[i]}$, $C^{[i]}$, $B_\omega^{[i]}$, $D_\upsilon^{[i]}$ are matrices of appropriate dimensions. $\theta$ is a vector that contains the uncertain parameters of the system that are assumed to be unknown but bounded. $A(\theta)$ is an uncertain matrix that can be defined as an interval matrix $[A]$.

This paper assumes that the initial state, process disturbance and measurement noise of the system are unknown but bounded as follows

$$\begin{aligned} x_0^{[i]} &\in \mathcal{X}_0^{[i]} = \left\langle p_0^{[i]}, H_0^{[i]} \right\rangle, \\ \omega_k^{[i]} &\in \mathcal{W}^{[i]} = \left\langle 0, H_\omega^{[i]} \right\rangle, \\ \upsilon_k^{[i]} &\in \mathcal{V}^{[i]} = \left\langle 0, H_\upsilon^{[i]} \right\rangle, \end{aligned} \tag{11}$$

where $\mathcal{X}_0^{[i]}$, $\mathcal{W}^{[i]}$ and $\mathcal{V}^{[i]}$ are the zonotopes bounding the initial state, process disturbance and measurement noise, respectively. The output zonotopes of the system can be obtained by propagating the uncertainty using the zonotope properties and the system model (10).

*Remark 1.* As discussed in[33], because of the parametric uncertainty, process disturbances and noise, there will always be a minimum fault size that will be not be detectable (i.e., the measured output will be in the healthy output set $\mathcal{Y}^{[0]}$ even in the fault presence) or isolable (i.e., $\mathcal{Y}^{[i]} \cap \mathcal{Y}^{[j]} \neq \emptyset, i \neq j, i, j \in \{1, 2, \cdots, q\}$).

To reduce the size of the minimum detectable/isolable faults, active FD based on the auxiliary input signal design relies on designing an auxiliary input signal, and injecting it into the system to improve the fault separability. Active FD based on set-membership approaches aims at designing auxiliary input signals to separate the output sets of different models, i.e.

$$\mathcal{Y}^{[i]} \cap \mathcal{Y}^{[j]} = \emptyset, i \neq j, i, j \in \{0, 1, 2, \cdots, q\}, \tag{12}$$

where $\mathcal{Y}^{[i]}$ and $\mathcal{Y}^{[j]}$ are the output sets of model $i$ and model $j$, respectively.

Figure 1 shows the process of active fault detection based on set-membership method. The healthy output set and faulty output set when the auxiliary input signal is not added to the system are shown in Figure 1(a). When the healthy and faulty models intersect, it is impossible to judge whether the system is faulty or not. When the optimal auxiliary input signal is injected into the system, the two sets are separated as shown in Figure 1(b).

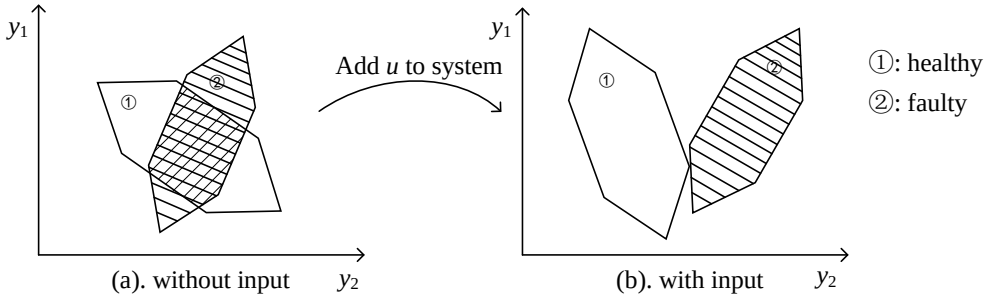


**FIGURE 1** Process of active fault detection.

The main objective of this paper is to design an optimal input signal such that the healthy output zonotope can be separated from the faulty output zonotope for discrete-time systems with parametric uncertainty.

## 3 | BOUNDING OUTPUT SET USING ZONOTOPIC OBSERVERS

The diagram of the approach proposed is this paper is depicted in Figure 2. In this figure, $u_{k-1}$ is the auxiliary input signal, $y_k$ is the system output, $\hat{x}_k^{[0]}$ and $\hat{x}_k^{[1]}$ are the state estimations obtained using the healthy and faulty models, respectively. $\mathcal{Y}_k^{[0]}$ and $\mathcal{Y}_k^{[1]}$ are the output zonotopes estimated using the healthy and faulty models, respectively. In order to reduce the conservativeness, a zonotopic observer is designed for estimating the output zonotope instead of using the systen model (10) as usually done in the active fault detection literature. Then, an auxiliary input signal is designed to separate the output zonotopes of the healthy model from the output zonotopes of the faulty model. Finally, the input signal is injected into the system to obtain the fault detection results.

The state observer mainly corrects the state of the system using the error between the measured output and the observed output. Therefore, the size of the output set is tighter by using a state observer leading to less conservative results that using the system model (10). In this section, a zonotopic observer is first designed for (10). Then, the size of the output zonotopes is analyzed and it is demonstrated that the zonotope size can be reduced with the proposed observer-based design method.

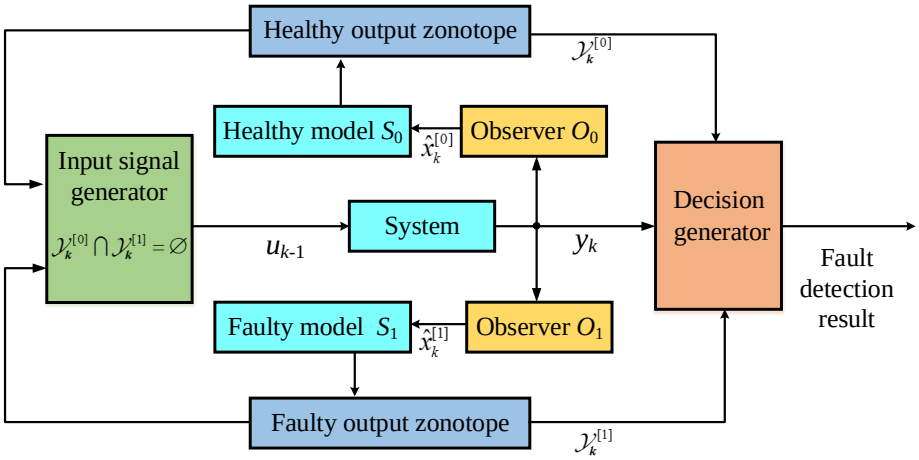


**FIGURE 2** Schematic diagram of the proposed approach.

## 3.1 | Zonotopic observer design

Based on the zonotopic Kalman filter approach[34], the observer for the system (10) has the following structure

$$\hat{x}_{k+1}^{[i]} = A^{[i]}(\theta)\hat{x}_k^{[i]} + B^{[i]}u_k + B_\omega^{[i]}\omega_k^{[i]} + L_k^{[i]}\left(y_k - C^{[i]}\hat{x}_k^{[i]} - D_\upsilon^{[i]}v_k^{[i]}\right), i = 0, 1, 2, \cdots, q. \tag{13}$$

where $\hat{x}_k^{[i]}$ is the estimate of the state at time $k$, $L_k^{[i]}$ is the time-varying observer gain and $y_k$ is the system output.

**Theorem 1.** Assume that the system state estimation at time sample $k$ satisfies $\hat{x}_k^{[i]} \in \mathcal{X}_k^{[i]} = \left\langle p_k^{[i]}, H_k^{[i]} \right\rangle$. Then, the state at sample time $k+1$ is given by

$$\hat{x}_{k+1}^{[i]} \in \mathcal{X}_{k+1}^{[i]} = \left\langle p_{k+1}^{[i]}, H_{k+1}^{[i]} \right\rangle, \tag{14}$$

where

$$\begin{cases} p_{k+1}^{[i]} = \mathrm{mid}([A^{[i]}] - L_k^{[i]}C^{[i]})p_k^{[i]} + B^{[i]}u_k + L_k^{[i]}y_k \\ H_{k+1}^{[i]} = \left[\mathrm{mid}([A^{[i]}] - L_k^{[i]}C^{[i]})\bar{H}_k^{[i]} \quad \mathrm{rs}(\mathrm{rad}([A^{[i]}] - L_k^{[i]}C^{[i]})\left|\bar{H}_k^{[i]}\right|), \right. \\ \qquad \left. \mathrm{rs}(\mathrm{rad}([A^{[i]}] - L_k^{[i]}C^{[i]})\left|p_k^{[i]}\right|) \quad B_\omega^{[i]}H_\omega^{[i]} \quad L_k^{[i]}D_\upsilon^{[i]}H_\upsilon^{[i]}\right], \end{cases} \tag{15}$$

$p_{k+1}^{[i]} \in \mathbb{R}^{n_x}$, $H_{k+1}^{[i]} \in \mathbb{R}^{n_x \times r_x}$, $\bar{H}_{k+1}^{[i]}$ represents the generator matrix after the zonotope reduction using Lemma 2 at sample time $k+1$.

*Proof.* According to (13) and taking into account the noise and disturbances bounds (11), the zonotope $\mathcal{X}_{k+1}^{[i]}$ can be rewritten as

$$\begin{aligned} \hat{x}_{k+1}^{[i]} \in \mathcal{X}_{k+1}^{[i]} =& [A^{[i]}]\mathcal{X}_k^{[i]} \oplus B^{[i]}u_k \oplus B_\omega^{[i]}\mathcal{W}^{[i]} \oplus L_k^{[i]}y_k \oplus (-L_k^{[i]}\mathcal{X}_k^{[i]}) \oplus (-L_k^{[i]}D_\upsilon^{[i]}\mathcal{V}^{[i]}) \\ =& \left[([A^{[i]}] - L_k^{[i]}C^{[i]}) \odot \left\langle p_k^{[i]}, H_k^{[i]} \right\rangle\right] \oplus B^{[i]}u_k \\ & \oplus L_k^{[i]}y_k \oplus \left[B_\omega^{[i]} \odot \left\langle 0, H_\omega^{[i]} \right\rangle\right] \oplus \left[(-L_k^{[i]}D_\upsilon^{[i]}) \odot \left\langle 0, H_\upsilon^{[i]} \right\rangle\right] \\ =& (([A^{[i]}] - L_k^{[i]}C^{[i]})p_k^{[i]} + B^{[i]}u_k + L_k^{[i]}y_k) \\ & \oplus \left[([A^{[i]}] - L_k^{[i]}C^{[i]})H_k^{[i]} \;\; B_\omega^{[i]}H_\omega^{[i]} \;\; L_k^{[i]}D_\upsilon^{[i]}H_\upsilon^{[i]}\right]. \end{aligned} \tag{16}$$

Using properties of the zonotope and Lemma 2, the center of the state zonotope and the generator matrix can be obtained at sample time $k+1$. □

In this paper, we mainly will use the output set that is consistent with the unknown but bounded parametric uncertainty, disturbances and noise. Then, from the zonotope that bounds the states (14), the zonotope that bounds the estimated output $\mathcal{Y}_{k+1}^{[i]}$ can be obtained using (13) as follows

$$\begin{aligned} y_{k+1}^{[i]} \in \mathcal{Y}_{k+1}^{[i]} &= C^{[i]}\mathcal{X}_{k+1}^{[i]} \oplus D_{\upsilon}^{[i]}\mathcal{V}^{[i]} \\ &= \left[C^{[i]} \odot \left\langle p_{k+1}^{[i]}, H_{k+1}^{[i]} \right\rangle\right] \oplus \left[D_{\upsilon}^{[i]} \odot \left\langle 0, H_{\upsilon}^{[i]} \right\rangle\right] \\ &= \left\langle C^{[i]} p_{k+1}^{[i]}, \left[C^{[i]} H_{k+1}^{[i]} \;\; D_{\upsilon}^{[i]} H_{\upsilon}^{[i]}\right] \right\rangle. \end{aligned} \tag{17}$$

Therefore, the center and radius of output zonotope can be obtained

$$\begin{cases} p_{y,k+1}^{[i]} = C^{[i]} p_{k+1}^{[i]}, \\ H_{y,k+1}^{[i]} = \left[C^{[i]} H_{k+1}^{[i]} \;\; D_{\upsilon}^{[i]} H_{\upsilon}^{[i]}\right], \end{cases} \tag{18}$$

where $p_{y,k+1}^{[i]} \in \mathbb{R}^{n_y}$, $H_{y,k+1}^{[i]} \in \mathbb{R}^{n_y \times r_y}$.

According to[29], given an observer such as (13), the optimal time-varying gain that minimizes the size of zonotope, measured by means of the Frobenius norm of the zontope segment matrix as

$$(J_{k+1}^{[i]})^2 = \mathrm{tr}((H_{k+1}^{[i]})^T H_{k+1}^{[i]}), \tag{19}$$

can be obtained as follows

$$\begin{aligned} L_k^{[i]} &= \mathrm{mid}([A^{[i]}])K_k^{[i]}, \\ K_k^{[i]} &= G_k^{[i]}(S_k^{[i]})^{-1}, \\ G_k^{[i]} &= P_k^{[i]}(C^{[i]})^T, \\ S_k^{[i]} &= C^{[i]} P_k^{[i]}(C^{[i]})^T + Q_{\upsilon}^{[i]}, \\ P_k^{[i]} &= \bar{H}_k^{[i]}(\bar{H}_k^{[i]})^T, \\ Q_{\upsilon}^{[i]} &= D_{\upsilon}^{[i]} H_{\upsilon}^{[i]}(H_{\upsilon}^{[i]})^T (D_{\upsilon}^{[i]})^T. \end{aligned} \tag{20}$$

The optimal gain (20) is derived considering that the size of the output zonotope (19) is minimized when $\frac{\partial (J_{k+1}^{[i]})^2}{\partial L_k^{[i]}} = 0$ based on the results in Combastel[35].

## 3.2 | Analysis of the size of output zonotopes

As previously discussed, the reduction of the size of the minimum detectable/isolable faults can be achieved by means of the design of the adequate auxiliary input signal such that the output zonotopes of the different models do not overlap. However, when the overlapping is important, the size of the auxiliary input signal to be used should be large to separate the output zonotope ofthe different models, disturbing the desired behaviour of the system. Therefore, in order to obtain a small auxiliary input signal, the size of the output zonotope should be as smaller as possible.

**Theorem 2.** Consider the system (10). The size of the output zonotope at time $k+1$, measured by means of (19), using the observer (13) with optimal gain (20) is smaller than the output zonotope obtained directly using the system model (10),

$$(J_{k+1})^2 \leq (\tilde{J}_{k+1})^2, \tag{21}$$

where $(J_{k+1})^2$ and $(\tilde{J}_{k+1})^2$ denote respectively the size of the output zonotope with and without observer.

*Proof.* The size of the output zonotope obtained with the observer can be measured by means of the Frobenius norm of the zonotope segment matrix (Property 5)

$$\begin{aligned}(J_{k+1})^2 =&\mathrm{tr}((H^{[i]}_{y,k+1})^T H^{[i]}_{y,k+1}) = \mathrm{tr}((\mathrm{mid}([A^{[i]}] - L^{[i]}_k C^{[i]})H^{[i]}_k)^T \mathrm{mid}([A^{[i]}] - L^{[i]}_k C^{[i]})H^{[i]}_k \\ &+ (\mathrm{rs}(\mathrm{rad}([A^{[i]}] - L^{[i]}_k C^{[i]}) \left|H^{[i]}_k\right|))^T \mathrm{rs}(\mathrm{rad}([A^{[i]}] - L^{[i]}_k C^{[i]}) \left|H^{[i]}_k\right|) \\ &+ (\mathrm{rs}(\mathrm{rad}([A^{[i]}] - L^{[i]}_k C^{[i]}) \left|p^{[i]}_k\right|))^T \mathrm{rs}(\mathrm{rad}([A^{[i]}] - L^{[i]}_k C^{[i]}) \left|p^{[i]}_k\right|) \\ &+ (B^{[i]}_\omega H^{[i]}_\omega)^T B^{[i]}_\omega H^{[i]}_\omega + (L^{[i]}_k D^{[i]}_\upsilon H^{[i]}_\upsilon)^T L^{[i]}_k D^{[i]}_\upsilon H^{[i]}_\upsilon).\end{aligned} \tag{22}$$

Using the properties of interval matrices, it follows that

$$\begin{aligned}&\mathrm{mid}([A^{[i]}] - L^{[i]}_k C^{[i]}) = \mathrm{mid}([A^{[i]}]) - L^{[i]}_k C^{[i]}, \\ &\mathrm{rad}([A^{[i]}] - L^{[i]}_k C^{[i]}) = \mathrm{rad}([A^{[i]}]).\end{aligned} \tag{23}$$

Therefore,

$$\begin{aligned}&(\mathrm{mid}([A^{[i]}] - L^{[i]}_k C^{[i]})H^{[i]}_k)^T \mathrm{mid}([A^{[i]}] - L^{[i]}_k C^{[i]})H^{[i]}_k \\ =&(H^{[i]}_k)^T (\mathrm{mid}([A^{[i]}]) - L^{[i]}_k C^{[i]})^T (\mathrm{mid}([A^{[i]}]) - L^{[i]}_k C^{[i]})H^{[i]}_k \\ =&(H^{[i]}_k)^T (\mathrm{mid}([A^{[i]}]))^T \mathrm{mid}([A^{[i]}])H^{[i]}_k - (H^{[i]}_k)^T (L^{[i]}_k C^{[i]})^T \mathrm{mid}([A^{[i]}])H^{[i]}_k \\ &- (H^{[i]}_k)^T (\mathrm{mid}([A^{[i]}]))^T L^{[i]}_k C^{[i]} H^{[i]}_k + (H^{[i]}_k)^T (L^{[i]}_k C^{[i]})^T L^{[i]}_k C^{[i]} H^{[i]}_k.\end{aligned} \tag{24}$$

We can proceed similarly to measure the size of output zonotope without observer

$$\begin{aligned}&(\tilde{J}_{k+1})^2 = \mathrm{tr}((\tilde{H}^{[i]}_{y,k+1})^T \tilde{H}^{[i]}_{y,k+1}) \\ =&\mathrm{tr}((\mathrm{mid}([A^{[i]}])\tilde{H}^{[i]}_k)^T \mathrm{mid}([A^{[i]}])\tilde{H}^{[i]}_k + (\mathrm{rs}(\mathrm{rad}([A^{[i]}]) \left|\tilde{H}^{[i]}_k\right|))^T \mathrm{rs}(\mathrm{rad}([A^{[i]}]) \left|\tilde{H}^{[i]}_k\right|) \\ &+ (\mathrm{rs}(\mathrm{rad}([A^{[i]}]) \left|\tilde{p}^{[i]}_k\right|))^T \mathrm{rs}(\mathrm{rad}([A^{[i]}]) \left|\tilde{p}^{[i]}_k\right|) + (B^{[i]}_\omega H^{[i]}_\omega)^T B^{[i]}_\omega H^{[i]}_\omega).\end{aligned} \tag{25}$$

In order to verify the size of output zonotope obtained by means of the observer (13) is smaller, the difference between (22) and (25) is evaluated

$$\begin{aligned}(J_{k+1})^2 - (\tilde{J}_{k+1})^2 =&\mathrm{tr}((L^{[i]}_k C^{[i]} H^{[i]}_k)^T L^{[i]}_k C^{[i]} H^{[i]}_k - (\mathrm{mid}([A^{[i]}])H^{[i]}_k)^T L^{[i]}_k C^{[i]} H^{[i]}_k \\ &- (L^{[i]}_k C^{[i]} H^{[i]}_k)^T \mathrm{mid}([A^{[i]}])H^{[i]}_k + (L^{[i]}_k D^{[i]}_\upsilon H^{[i]}_\upsilon)^T L^{[i]}_k D^{[i]}_\upsilon H^{[i]}_\upsilon).\end{aligned} \tag{26}$$

Considering the observer optimal gain (20), previous equation can be rewritten

$$(J_{k+1})^2 - (\tilde{J}_{k+1})^2 = -\mathrm{tr}(L^{[i]}_k C^{[i]} H^{[i]}_k (H^{[i]}_k)^T (C^{[i]})^T (L^{[i]}_k)^T) - \mathrm{tr}(L^{[i]}_k Q^{[i]}_\upsilon (L^{[i]}_k)^T), \tag{27}$$

where $Q^{[i]}_\upsilon = D^{[i]}_\upsilon H^{[i]}_\upsilon (D^{[i]}_\upsilon H^{[i]}_\upsilon)^T$.

Since $L^{[i]}_k C^{[i]} H^{[i]}_k (H^{[i]}_k)^T (C^{[i]})^T (L^{[i]}_k)^T$ and $L^{[i]}_k Q^{[i]}_\upsilon (L^{[i]}_k)^T$ are symmetric matrices with positive elements, it follows that

$$(J_{k+1})^2 - (\tilde{J}_{k+1})^2 \leq 0, \tag{28}$$

Therefore, Theorem 2 is proved. □

In summary, since the size of the output zonotope is reduced by using an observer-based method, the auxiliary input signal designed by the optimal zonotopic observer method will be smaller. The optimal input signal will be obtained by forcing that the intersection of the output zonotopes in the different system modes is empty. The injection of this signal into the system will allow reducing the size of the minimum separable faults.

## 4 | OPTIMAL AUXILIARY INPUT DESIGN

In this section, an optimal auxiliary input signal is designed by using the output sets determined in previous section. Since the addition of the input signal will affect the system, the input signal is required to be minimized such that small faults could be detected. In this section, the problem of solving the optimal auxiliary input signal design is mainly transformed into the problem of solving the mixed integer quadratic programming (MIQP).

The optimal auxiliary input signal should satisfy

$$\begin{aligned} &\min_{u_k} (u_k)^T R u_k \\ &s.t. \quad \mathcal{Y}_{k+1}^{[i]} \cap \mathcal{Y}_{k+1}^{[j]} = \varnothing, i \neq j, i, j \in \{0, 1, 2, \cdots, q\}. \end{aligned} \tag{29}$$

where $R$ is a positive semi-definite matrix.

According to (18), the output zonotope is given by

$$\begin{aligned} \mathcal{Y}_{k+1}^{[i]} &= \left\langle p_{y,k+1}^{[i]}, H_{y,k+1}^{[i]} \right\rangle \\ &= C^{[i]}([A^{[i]}] - L_k^{[i]} C^{[i]}) \mathcal{X}_k^{[i]} \oplus C^{[i]} B^{[i]} u_k \oplus C^{[i]} L_k^{[i]} y_k \oplus C^{[i]} B_\omega^{[i]} \mathcal{W}^{[i]} \oplus (-C^{[i]} L_k^{[i]} D_v^{[i]} \mathcal{V}^{[i]}). \end{aligned} \tag{30}$$

that can be expressed as

$$\mathcal{Y}_{k+1}^{[i]} = \mathcal{M}_k^{[i]} + C^{[i]} B^{[i]} u_k = \left\langle \bar{p}_{y,k+1}^{[i]} + C^{[i]} B^{[i]} u_k, H_{y,k+1}^{[i]} \right\rangle, \tag{31}$$

with

$$\mathcal{M}_k^{[i]} = \left\langle \bar{p}_{y,k+1}^{[i]}, H_{y,k+1}^{[i]} \right\rangle, \tag{32}$$

where

$$\begin{aligned} \bar{p}_{y,k+1}^{[i]} &= C^{[i]} \mathrm{mid}([A^{[i]}] - L_k^{[i]} C^{[i]}) p_k^{[i]} + L_k{}^{[i]} y_k, \\ p_{y,k+1}^{[i]} &= \bar{p}_{y,k+1}^{[i]} + C^{[i]} B^{[i]} u_k. \end{aligned} \tag{33}$$

**Theorem 3.** The intersection of output zonotopes of the healthy and faulty models is empty

$$\mathcal{Y}_{k+1}^{[i]} \cap \mathcal{Y}_{k+1}^{[j]} = \varnothing, i \neq j, i, j \in \{0, 1, 2, \cdots, q\}. \tag{34}$$

if and only if

$$\triangle^{[ij]} u_k \notin \mathcal{Y}_{m,k}^{[ij]}, \tag{35}$$

where $\triangle^{[ij]} = C^{[j]} B^{[j]} - C^{[i]} B^{[i]}$, $\mathcal{Y}_{m,k}^{[ij]} = \mathcal{M}_k^{[i]} - \mathcal{M}_k^{[j]}$.

*Proof.* Using (32), (34) can be written as

$$\left\langle \bar{p}_{y,k+1}^{[i]} + C^{[i]} B^{[i]} u_k, H_{y,k+1}^{[i]} \right\rangle \cap \left\langle \bar{p}_{y,k+1}^{[j]} + C^{[j]} B^{[j]} u_k, H_{y,k+1}^{[j]} \right\rangle = \varnothing. \tag{36}$$

According to Lemma 3, if and only if

$$C^{[j]} B^{[j]} u_k - C^{[i]} B^{[i]} u_k \notin \left\langle \bar{p}_{y,k+1}^{[i]}, H_{y,k+1}^{[i]} \right\rangle \oplus \left\langle -\bar{p}_{y,k+1}^{[j]}, H_{y,k+1}^{[j]} \right\rangle = \mathcal{M}_k^{[i]} - \mathcal{M}_k^{[j]}. \tag{37}$$

Theorem 3 is proved. □

So, according to Theorem 3, (29) can be rewritten as

$$\begin{aligned} &\min_{u_k} (u_k)^T R u_k \\ &s.t. \quad \triangle^{[ij]} u_k \notin \mathcal{Y}_{m,k}^{[ij]}, i \neq j, i, j \in \{0, 1, 2, \cdots, q\}. \end{aligned} \tag{38}$$

Since optimization problem (38) is a non-convex optimization problem, it is not easy to obtain the optimal solution. So, the optimization problem (38) is reformulated and transformed into a MIQP problem to obtain the effective solution.

To this aim, the zonotope $\mathcal{Y}_{m,k}^{[ij]}$ is defined as

$$\mathcal{Y}_{m,k}^{[ij]} = \left\langle p_{m,k}^{[ij]}, H_{m,k}^{[ij]} \right\rangle, \tag{39}$$

where $p_{m,k}^{[ij]} \in \mathbb{R}^{n_y}$, $H_{m,k}^{[ij]} \in \mathbb{R}^{n_y \times 2r_y}$. When $H_{m,k}^{[ij]}$ is a row full rank matrix, $\mathcal{Y}_{m,k}^{[ij]}$ is a non-empty set.

Using Definition 1, when $\triangle^{[ij]} u_k \in \mathcal{Y}_{m,k}^{[ij]}$,

$$\triangle^{[ij]} u_k = p_{m,k}^{[ij]} + H_{m,k}^{[ij]} \alpha'^{[ij]}, \tag{40}$$

where $\left\| \alpha'^{[ij]} \right\|_\infty \leq 1$. If $\triangle^{[ij]} u_k \notin \mathcal{Y}_{m,k}^{[ij]}$,

$$\triangle^{[ij]} u_k = p_{m,k}^{[ij]} + H_{m,k}^{[ij]} \alpha^{[ij]}, \tag{41}$$

where $\left\|\alpha^{[ij]}\right\|_\infty \leq 1+\varepsilon^{[ij]}$ and $\varepsilon^{[ij]} > 0$.

Therefore, (34) can be rewritten as

$$\begin{aligned}
&\min_{u_k} (u_k)^T R u_k \\
&\min_{\varepsilon^{[ij]},\alpha^{[ij]}} \varepsilon^{[ij]} \\
&s.t. \quad \triangle^{[ij]} u_k = H_{m,k}^{[ij]} \alpha^{[ij]} + p_{m,k}^{[ij]}, \\
&\qquad \left\|\alpha^{[ij]}\right\|_\infty \leq 1+\varepsilon^{[ij]}, \\
&\qquad \varepsilon^{[ij]} > 0, \quad i \neq j, i, j \in \{0,1,2,\cdots,q\}.
\end{aligned} \tag{42}$$

Note that the feasible set in (34) is an unbounded set due to the constraint $\varepsilon^{[ij]} > 0$ in (42). Therefore, in order to obtain the optimal auxiliary input signal $u_k$, suppose there is an upper bound $\bar{\varepsilon}^{[ij]}$ and a lower bound $\underline{\varepsilon}^{[ij]}$, i.e.

$$\underline{\varepsilon}^{[ij]} \leq \varepsilon^{[ij]} \leq \bar{\varepsilon}^{[ij]}. \tag{43}$$

where $\underline{\varepsilon}^{[ij]} > 0$ and $\bar{\varepsilon}^{[ij]}$ are established according to the physical knowledge of the particular system.

Using (43), (42) can be rewritten as the following two-layer optimization problem

$$\begin{aligned}
&\min_{u_k} (u_k)^T R u_k \\
&\min_{\varepsilon^{[ij]},\alpha^{[ij]}} \varepsilon^{[ij]} \\
&s.t. \quad \underline{\varepsilon}^{[ij]} \leq \varepsilon^{[ij]} \leq \bar{\varepsilon}^{[ij]}, \\
&\qquad \triangle^{[ij]} u_k = H_{m,k}^{[ij]} \alpha^{[ij]} + p_{m,k}^{[ij]}, \\
&\qquad \left\|\alpha^{[ij]}\right\|_\infty \leq 1+\varepsilon^{[ij]}, \\
&\qquad \varepsilon^{[ij]} > 0, \quad i \neq j, i, j \in \{0,1,2,\cdots,q\}.
\end{aligned} \tag{44}$$

This two-layer optimization problem is not easy to be solved. Using the Theorem 3.3.1 and Theorem 3.4.1 in the book[36], the two-layer optimization problem in (44) can be transformed into a single-layer optimization problem by constructing a Lagrangian function.

**Theorem 4.** For system (10) and using the zonotopic observer in Theorem 1, the optimal auxiliary input signal can be obtained by solving the following optimization problem

$$\begin{aligned}
&\min_{u_k} (u_k)^T R u_k \\
&s.t. \quad \underline{\varepsilon}^{[ij]} \leq \varepsilon^{[ij]} \leq \bar{\varepsilon}^{[ij]}, \\
&\qquad \triangle^{[ij]} u_k = H_{m,k}^{[ij]} \alpha^{[ij]} + p_{m,k}^{[ij]}, \\
&\qquad \left\|\alpha^{[ij]}\right\|_\infty \leq 1+\varepsilon^{[ij]}, \\
&\qquad (\mu_1^{[ij]} + \mu_2^{[ij]})^T \mathbf{1} = 1, \\
&\qquad \mu_1^{[ij]} - \mu_2^{[ij]} = (H_{m,k}^{[ij]})^T \lambda^{[ij]}, \\
&\qquad (\alpha^{[ij]} - 1 - \varepsilon_l^{[ij]}) \in [-2(1+\bar{\varepsilon}^{[ij]})(1-b_{1,l}^{[ij]}), 0], \\
&\qquad (\alpha^{[ij]} + 1 + \varepsilon_l^{[ij]}) \in [0, 2(1+\bar{\varepsilon}^{[ij]})(1-b_{2,l}^{[ij]})], \\
&\qquad l = 1,2,\cdots,2r_y, \varepsilon^{[ij]} > 0,\ i \neq j, i, j \in \{0,1,2,\cdots,q\}.
\end{aligned} \tag{45}$$

where $\lambda^{[ij]}$, $\mu_1^{[ij]}$ and $\mu_2^{[ij]}$ are the Lagrange multipliers, vector $\mathbf{1}=\begin{bmatrix}1 & 1 & \cdots & 1\end{bmatrix} \in \mathbb{R}^{2r_y}$, $b_{1,l}^{[ij]}$ and $b_{2,l}^{[ij]}$ are binary variables. $\mu_1^{[ij]}$ and $\mu_2^{[ij]}$ respectively satisfy

$$\mu_1^{[ij]} = \begin{bmatrix}\mu_{1,1}^{[ij]} & \mu_{1,2}^{[ij]} & \cdots & \mu_{1,2r_y}^{[ij]}\end{bmatrix}^{\mathrm{T}} \in \mathbb{R}^{2r_y}, \tag{46}$$

and

$$\mu_2^{[ij]} = \begin{bmatrix}\mu_{2,1}^{[ij]} & \mu_{2,2}^{[ij]} & \cdots & \mu_{2,2r}^{[ij]}\end{bmatrix}^{\mathrm{T}} \in \mathbb{R}^{2r_y}, \tag{47}$$

*Proof.* The Lagrange function for the optimization problem (45) is

$$\begin{aligned}\mathcal{L} =&\varepsilon^{[ij]} + \lambda^{[ij]}(H_{m,k}^{[ij]}\alpha^{[ij]} + p_{m,k}^{[ij]} - \triangle^{[ij]}u_k) + \mu_{1,1}^{[ij]}(-\alpha_1^{[ij]} - 1 - \varepsilon^{[ij]}) + \mu_{1,2}^{[ij]}(-\alpha_2^{[ij]} - 1 - \varepsilon^{[ij]}) + \cdots \\ &+ \mu_{2,2r_y}^{[ij]}(-\alpha_{2r_y}^{[ij]} - 1 - \varepsilon^{[ij]}) + \mu_{1,1}^{[ij]}(\alpha_1^{[ij]} - 1 - \varepsilon^{[ij]}) + \mu_{2,2}^{[ij]}(\alpha_2^{[ij]} - 1 - \varepsilon^{[ij]}) + \cdots + \mu_{2,2r_y}^{[ij]}(\alpha_{2r_y}^{[ij]} - 1 - \varepsilon^{[ij]}) \\ =&\varepsilon^{[ij]} + \lambda^{[ij]}(H_{m,k}^{[ij]}\alpha^{[ij]} + p_{m,k}^{[ij]} - \triangle^{[ij]}u_k) - (\mu_1^{[ij]})^T\alpha^{[ij]} - (\mu_1^{[ij]})^T\mathbf{1} - (\mu_1^{[ij]})^T\mathbf{1}\varepsilon^{[ij]} \\ &+ (\mu_2^{[ij]})^T\alpha^{[ij]} - (\mu_2^{[ij]})^T\mathbf{1} - (\mu_2^{[ij]})^T\mathbf{1}\varepsilon^{[ij]}.\end{aligned} \tag{48}$$

The first-order optimally conditions can be obtained by computing the derivative of $\mathcal{L}$ with respect the decision variables

$$\begin{aligned}&\frac{\partial\mathcal{L}}{\partial\varepsilon^{[ij]}} = 1 - (\mu_1^{[ij]} + \mu_2^{[ij]})^T\mathbf{1} = 0, \\ &\frac{\partial\mathcal{L}}{\partial\varepsilon^{[ij]}} = (H_{m,k}^{[ij]})^T - \mu_1^{[ij]} + \mu_2^{[ij]} = 0, \\ &\mu_{1,l}^{[ij]}(\alpha_l^{[ij]} - 1 - \varepsilon^{[ij]})=0, \\ &\mu_{2,l}^{[ij]}(\alpha_1^{[ij]} + 1 + \varepsilon^{[ij]}) = 0.\end{aligned} \tag{49}$$

The constraints $\mu_{1,l}^{[ij]}(\alpha_l^{[ij]} - 1 - \varepsilon^{[ij]}) = 0$ and $\mu_{2,l}^{[ij]}(\alpha_l^{[ij]} + 1 + \varepsilon^{[ij]}) = 0$ are reformulated by introducing binary variables $b_1^{[ij]}, b_2^{[ij]} \in \{0, 1\}$ as follows

$$\begin{aligned}&b_{1,l}^{[ij]} = 1 \Rightarrow \mu_{1,l}^{[ij]}, \text{free}, \quad (\alpha^{[ij]} - 1 - \varepsilon_l^{[ij]}) = 0, \\ &b_{1,l}^{[ij]} = 0 \Rightarrow \mu_{1,l}^{[ij]} = 0, \quad (\alpha^{[ij]} - 1 - \varepsilon_l^{[ij]}), \text{free}, \\ &b_{2,l}^{[ij]} = 1 \Rightarrow \mu_{2,l}^{[ij]}, \text{free}, \quad (\alpha^{[ij]} + 1 + \varepsilon_l^{[ij]}) = 0, \\ &b_{2,l}^{[ij]} = 0 \Rightarrow \mu_{2,l}^{[ij]} = 0, \quad (\alpha^{[ij]} + 1 + \varepsilon_l^{[ij]}), \text{free}.\end{aligned} \tag{50}$$

Therefore, (50) can be written as

$$\begin{aligned}&\mu_{1,l}^{[ij]}\ ,\ \mu_{2,l}^{[ij]} \in [0, 1], \\ &(\alpha^{[ij]} - 1 - \varepsilon_l^{[ij]}) \in [-2(1 + \bar{\delta}^{[ij]}), 0], \\ &(\alpha^{[ij]} + 1 + \varepsilon_l^{[ij]}) \in [0, 2(1 + \bar{\delta}^{[ij]})],\end{aligned} \tag{51}$$

that after some manipulation can be expressed as the following linear constraints:

$$\begin{aligned}&\mu_{1,l}^{[ij]} \le b_{1,l}^{[ij]}\ ,\ \mu_{2,l}^{[0i]} \le b_{2,l}^{[ij]}, \\ &(\alpha^{[ij]} - 1 - \varepsilon_l^{[ij]}) \in [-2(1 + \bar{\varepsilon}^{[ij]})(1 - b_{1,l}^{[ij]}), 0], \\ &(\alpha^{[ij]} + 1 + \varepsilon_l^{[ij]}) \in [0, 2(1 + \bar{\varepsilon}^{[ij]})(1 - b_{2,l}^{[ij]})].\end{aligned} \tag{52}$$

More details of this proof process can be seen in the Scott's work[31]. □

*Remark 2.* Assume that the system is stable similarly as considered in the Zhai's and Scott's works[18,31]. Thus, as an additional input signal, auxiliary input will not affect the stability of the system.

When the auxiliary input signal is obtained, the logic of active FD is mainly based on determining whether the output of the actual system is faulty, then the problem can be transformed into:

$$\text{Fault detection results} = \begin{cases} 1 & y_k \in \mathcal{Y}_k^{[0]}, \\ -1 & y_k \in \mathcal{Y}_k^{[i]}, \\ 0 & y_k \notin \mathcal{Y}_k^{[0]} \text{ and } y_k \notin \mathcal{Y}_k^{[i]}. \end{cases} \tag{53}$$

where $\mathcal{Y}_k^{[0]}$ and $\mathcal{Y}_k^{[i]}$ correspond to the output zonotopes in healthy and faulty models, respectively. If $y_k$ is inside the healthy output zonotope, we use 1 to represent the fault detection result, which means that the system is healthy operation. If $y_k$ falls into faulty output zonotope, $-1$ is used to represent that the system is faulty. However, sometimes the system is in the transient state from healthy to faulty, $y_k$ belongs neither to the healthy output zonotope nor the faulty output zonotope at a particular time instant. Consequently, it can not be decided whether the system is faulty or not, we use 0 to represent this situation.

*Remark 3.* Assuming that there is a point $x \in \mathbb{R}^n$ and zonotope $\mathcal{X} = p \oplus H\mathbf{B}^r$, where $p \in \mathbb{R}^n$, $H \in \mathbb{R}^{n\times r}$. According to the properties of zonotope, the problem of determining whether a point belongs to a zonotope can be transformed into the following

**Algorithm 1** Active fault detection based on zonotope for uncertain systems

Given $A^{[i]}(\theta)$, $B^{[i]}$, $C^{[i]}$, $B_{\omega}^{[i]}$, $D_{v}^{[i]}$, $\mathcal{W}^{[i]}$ and $\mathcal{V}^{[i]}$, $i = 0, 1, \cdots, q$;
$\mathcal{X}_{k-1}^{[i]} \Leftarrow \mathcal{X}_{0}^{[i]}$, $y_{k-1} \Leftarrow y_0$;
**for** $k = 1$ to end **do**
  Obtain the optimal observer gain $L_{k-1}^{[i]}$;
  Compute $p_{m,k-1}^{[0i]}$ and $H_{m,k-1}^{[0i]}$ according to (32);
  Obtain $u_{k-1}$ by the Theorem 4, than inject it into the system (10);
  Measure $y_k$;
  Compute the healthy output zonotope $\mathcal{Y}_{k}^{[0]}$ and the faulty output zonotope $\mathcal{Y}_{k}^{[i]}$ of system respectively by using (17);
  **if** $y_k \in \mathcal{Y}_{k}^{[0]}$ **then**
    Fault detection results = 1, the system is healthy;
    **if** $y_k \in \mathcal{Y}_{k}^{[i]}$ **then**
      Fault detection results =-1, the system is faulty;
    **else**
      Fault detection results = 0, it can not be decided whether the system is faulty or not.
    **end if**
  **end if**
**end for**

constraints:

$$\begin{cases} p_1 + H_1\alpha = x_1, \\ p_2 + H_2\alpha = x_2, \\ \quad\vdots \\ p_n + H_n\alpha = x_{n_x}, \end{cases} \tag{54}$$

where $\alpha$=$[\alpha_1 \ \alpha_2 \ \cdots \ \alpha_r]^T$ . Constraints (54) hold if and only if $\|\alpha_r\| \leq 1$. So, when $x$ satisfies the constraints (54), it means that $x$ belongs to the zonotope $\mathcal{X}$.

Thus, according to Remark 4, the verification of the fault detection conditions presented in (53) can be implemented by solving the constraint satisfaction problem (54). As a result, the proposed active FD method is summarized in Algorithm 1.

## 5 | SIMULATION

The low-frequency linear model of a permanent magnet DC motor[31] is used to verify the effectiveness of the proposed method in this paper. The expression of the model is as follows

$$\begin{aligned} \begin{bmatrix} \frac{di_m(t)}{dt} \\ \\ \frac{dn_m(t)}{dt} \end{bmatrix} &= \begin{bmatrix} -\frac{R}{L} & -\frac{M_e}{L} \\ \\ \frac{M_t}{J_1} & -\frac{f_r}{J_1} \end{bmatrix} \begin{bmatrix} i_m(t) \\ \\ n_m(t) \end{bmatrix} + \begin{bmatrix} \frac{1}{L} \\ \\ 0 \end{bmatrix} u(t), \\ \begin{bmatrix} y_1(t) \\ y_2(t) \end{bmatrix} &= \begin{bmatrix} 1 & 0 \\ 0 & 1 \end{bmatrix} \begin{bmatrix} x_1(t) \\ x_2(t) \end{bmatrix}, \end{aligned} \tag{55}$$

where $i_m$(A), $u$(V), $R$(Ω), $L$(H), $M_e$(V rad/s), $M_t$(N m/amp), $J_1$(J s$^2$/rad) and $f_r$(J s/rad) are current, armature voltage, resistance, inductance, back EMF constant, torque constant, motor inertia and friction coefficient, respectively. The parameters of the model are shown in Table 1.

**TABLE 1** Model parameters.

| **model**($i$) | $R$ | $L(10^{-3})$ | $M_e(10^{-2})$ | $J_1(10^{-4})$ | $f_r(10^{-4})$ |
|---|---|---|---|---|---|
| 0 | 1.2030 | 5.5840 | 8.1876 | 1.3528 | 2.3396 |
| 1 | 1.2030 | 8.7548 | 8.1876 | 1.3528 | 2.3396 |

The torque constant $M_t$ can be obtained from the back EMF constant $M_e$ as follows: $M_t = 1.0005 M_e$. In order to operate the motor at the speed to 70.3(rad/s), the control input $u_c = 6$ V is applied.

The Euler method is used to discretize (55). Considering the model uncertainties and after time discretization, the discrete-time linear model is obtained as follows

$$\begin{cases} x_{k+1} = A(\theta)x_k + Bu_k + B_\omega \omega_k, \\ y_k = Cx_k + D_\upsilon \upsilon_k, \end{cases} \tag{56}$$

where

$$A(\theta) \triangleq [A] = A + \Theta, \tag{57}$$

and $\Theta = \begin{bmatrix} \theta & 0 \\ 0 & \theta \end{bmatrix}$ is uncertain matrix, $|\theta| \leq 0.03$. When the system is in the model $i = 0$, the system is healthy operation

$$A^{[0]} = \begin{bmatrix} 0.286 & -0.043 \\ 1.771 & 0.914 \end{bmatrix},\ B^{[0]} = \begin{bmatrix} 0.529 & 0.953 \end{bmatrix},\ C^{[0]} = \begin{bmatrix} 1 & 0 \\ 0 & 1 \end{bmatrix},\ B_\omega^{[0]} = \begin{bmatrix} -0.0254 & -0.0778 \\ -0.3996 & 0.3026 \end{bmatrix},\ D_\upsilon^{[0]} = \begin{bmatrix} 1 & 0 \\ 0 & 1 \end{bmatrix}.$$

When a fault occurs, the parameter matrices of the system are

$$A^{[1]} = \begin{bmatrix} 0.459 & -0.033 \\ 2.121 & 0.936 \end{bmatrix},\ B^{[1]} = \begin{bmatrix} 0.404 & 0.684 \end{bmatrix},\ C^{[1]} = \begin{bmatrix} 1 & 0 \\ 0 & 1 \end{bmatrix},\ B_\omega^{[1]} = \begin{bmatrix} -0.0254 & -0.0778 \\ -0.3996 & 0.3026 \end{bmatrix},\ D_\upsilon^{[1]} = \begin{bmatrix} 1 & 0 \\ 0 & 1 \end{bmatrix}.$$

The simulation results presented in the following are obtained considering that the initial state, measurement noise, and process disturbance of the system satisfy the following bounds

$$\begin{aligned} \boldsymbol{x}_0 &\in \mathcal{X}_0 = \left\langle \begin{bmatrix} 0.6 \\ 70 \end{bmatrix} \begin{bmatrix} 0.06 & 0 \\ 0 & 0.6 \end{bmatrix} \right\rangle, \\ \boldsymbol{\upsilon}_k &\in \mathcal{V} = \left\langle \begin{bmatrix} 0 \\ 0 \end{bmatrix} \begin{bmatrix} 0.06 & 0 \\ 0 & 0.6 \end{bmatrix} \right\rangle, \\ \boldsymbol{w}_k &\in \mathcal{W} = \langle \mathbf{0}, I_2 \rangle. \end{aligned} \tag{58}$$

Assume that the actual system is operating as follows

$$\text{system} = \begin{cases} \text{healthy} & 0 \leq k < 20, \\ \text{faulty} & 20 \leq k < 40, \\ \text{healthy} & 40 \leq k < 60. \end{cases} \tag{59}$$

Figure 3 shows the output sets of healthy and faulty in case that auxiliary input signal is not used. In this figure, the red zonotopes and the blue zonotopes are the output sets of the healthy and the faulty models, respectively. Black circles represent the output of actual system. When the auxiliary input signal is not injected into the system, the output set of the healthy model intersects with the output set of the faulty model. When the actual system belongs to the intersecting part, it is impossible to detect whether the fault has occurred. Therefore, in order to detect faults in the system, a proper auxiliary input signal is needed to separate the healthy output sets from the faulty output sets.

In order to verify the effectiveness of the proposed method, the additional methods are used for comparison.

- Method ①: Considering system parameter uncertainties, auxiliary input signal is generated based on output zonotopes without observers.

  For system (10), it is assumed that the state at sample time $k$ is $\tilde{x}_k^{[i]} \in \tilde{\mathcal{X}}_k^{[i]} = \left\langle \tilde{p}_k^{[i]}, \tilde{H}_k^{[i]} \right\rangle$. The state at sample time $k+1$ is

$$\tilde{x}_{k+1}^{[i]} \in \tilde{\mathcal{X}}_{k+1}^{[i]} = \left\langle \tilde{p}_{k+1}^{[i]}, \tilde{H}_{k+1}^{[i]} \right\rangle, \tag{60}$$

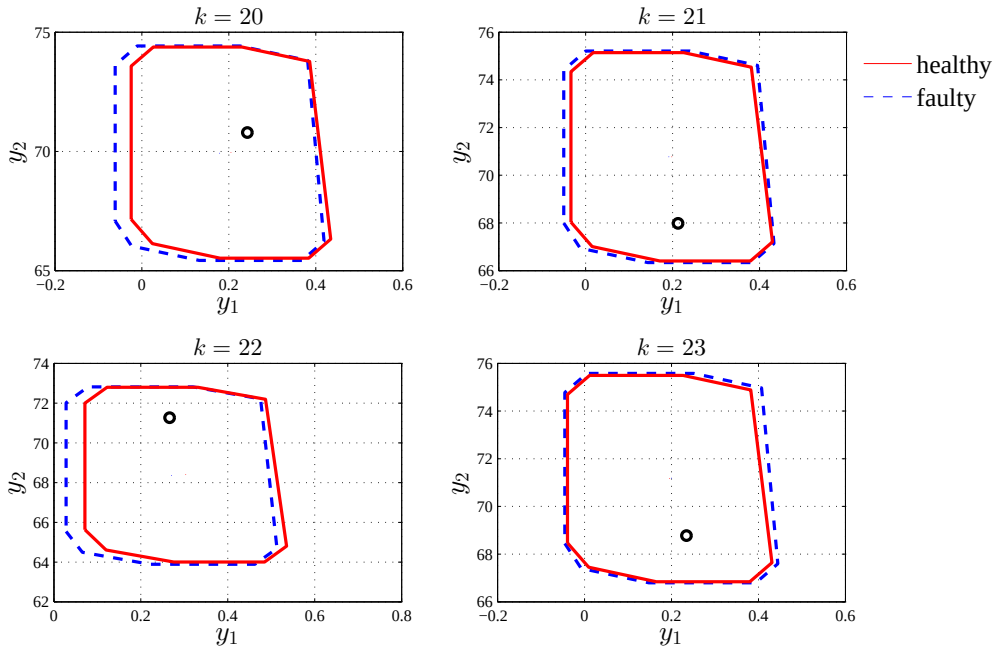


**FIGURE 3** The output sets of healthy and faulty without auxiliary input signal.

where

$$\begin{cases} \tilde{p}_{k+1}^{[i]} = \text{mid}([A^{[i]}])\tilde{p}_k^{[i]} + B^{[i]}u_k, \\ \tilde{H}_{k+1}^{[i]} = \left[\text{mid}([A^{[i]}])\tilde{H}_k^{[i]} \;\; \text{rs}(\text{rad}([A^{[i]}]))\left|\tilde{H}_k^{[i]}\right| \;\; \text{rs}(\text{rad}([A^{[i]}]))\left|\tilde{p}_k^{[i]}\right| \;\; B_\omega^{[i]}H_\omega^{[i]}\right]. \end{cases} \tag{61}$$

Therefore, the zonotope of output system is

$$\tilde{y}_{k+1}^{[i]} \in \tilde{\mathcal{Y}}_{k+1}^{[i]} = \left\langle \tilde{p}_{k+1}^{[i]}, \tilde{H}_{y,k+1}^{[i]} \right\rangle, \tag{62}$$

where

$$\begin{cases} \tilde{p}_{y,k+1}^{[i]} = C^{[i]}\tilde{p}_k^{[i]}, \\ \tilde{H}_{y,k+1}^{[i]} = \left[C^{[i]}\tilde{H}_{k+1}^{[i]} \;\; D_v^{[i]}H_v^{[i]}\right]. \end{cases} \tag{63}$$

- Method ②: Observer-based fault detection method without considering system parameter uncertainties.

Assuming that the state at sample time $k$ is $\tilde{\tilde{x}}_k^{[i]} \in \tilde{\tilde{\mathcal{X}}}_k^{[i]} = \left\langle \tilde{\tilde{p}}_k^{[i]}, \tilde{\tilde{H}}_k^{[i]} \right\rangle$. The state at sample time $k+1$ is

$$\tilde{\tilde{x}}_{k+1}^{[i]} \in \tilde{\tilde{\mathcal{X}}}_{k+1}^{[i]} = \left\langle \tilde{\tilde{p}}_{k+1}^{[i]}, \tilde{\tilde{H}}_{k+1}^{[i]} \right\rangle, \tag{64}$$

where

$$\begin{cases} \tilde{\tilde{p}}_{k+1}^{[i]} = (A^{[i]} - L_k^{[i]}C^{[i]})\tilde{\tilde{p}}_k^{[i]} + B^{[i]}u_k + L_k^{[i]}y_k, \\ \tilde{\tilde{H}}_{k+1}^{[i]} = \left[(A^{[i]} - L_k^{[i]}C^{[i]})\tilde{\tilde{H}}_k^{[i]} \;\; B_\omega^{[i]}H_\omega^{[i]} \;\; L_k^{[i]}D_v^{[i]}H_v^{[i]}\right]. \end{cases} \tag{65}$$

Therefore, the zonotope of output system can be written as

$$\tilde{\tilde{y}}_{k+1}^{[i]} \in \tilde{\tilde{\mathcal{Y}}}_{k+1}^{[i]} = \left\langle \tilde{\tilde{p}}_{y,k+1}^{[i]}, \tilde{\tilde{H}}_{y,k+1}^{[i]} \right\rangle, \tag{66}$$

where

$$\begin{cases} \tilde{\tilde{p}}_{y,k+1}^{[i]} = C^{[i]}\tilde{\tilde{p}}_k^{[i]}, \\ \tilde{\tilde{H}}_{y,k+1}^{[i]} = \left[C^{[i]}\tilde{\tilde{H}}_{k+1}^{[i]} \;\; D_v^{[i]}H_v^{[i]}\right]. \end{cases} \tag{67}$$

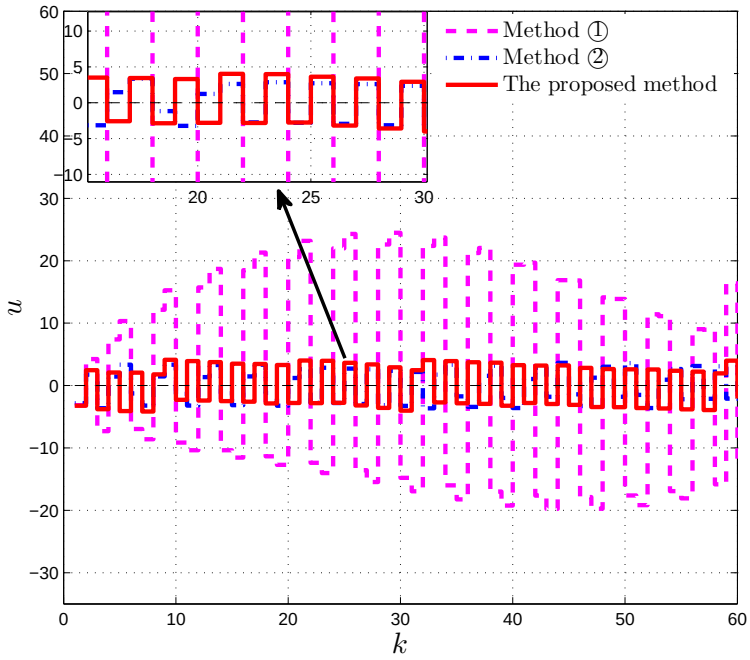


**FIGURE 4** The auxiliary input signal.

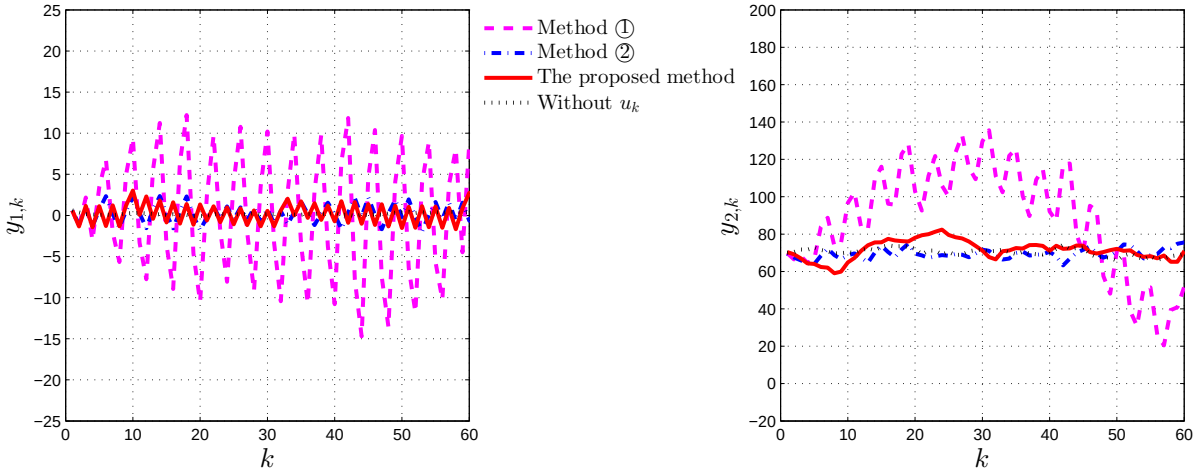


**FIGURE 5** The effect of auxiliary input signal on system output.

Figures 4−6 show the size of the generated input signals, the influence of the auxiliary input signal on system and the size of the output zonotope with the method ①, method ② and the proposed method, respectively. In Figure 4, the purple dashed line, blue dotted line and red solid line are the auxiliary input signals obtained by method ①, method ② and the proposed method, respectively. The amplitudes of auxiliary input signals by method ② and the proposed method are smaller than method ①. Also, it can be seen that the influence of the input signals based on Method ① is largest then the other two. The size of the output zonotope can be obtained by means of Property 6. According to the idea of active FD, the larger the volume of the output zonotopes, the greater volume of the intersection of the output zonotopes, so a larger auxiliary input signal is required to separate them. In Figure 6, $V_1$ and $V_2$ represent the size of the output zonotopes in healthy and faulty models, respectively.

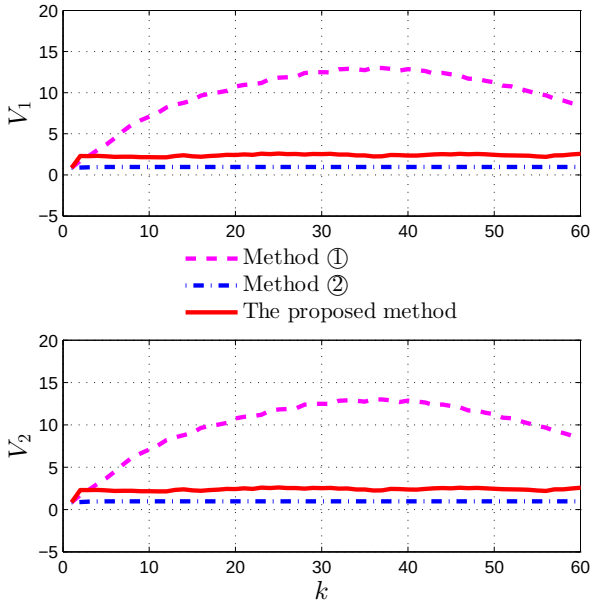


**FIGURE 6** The size of zonotope.

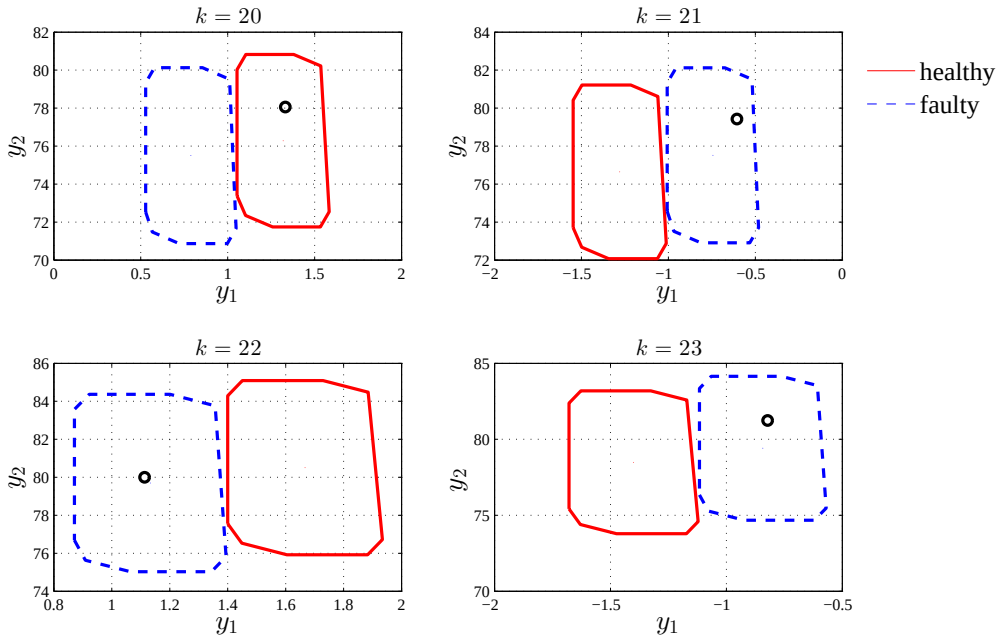


**FIGURE 7** The output sets of healthy and faulty obtained by the proposed method model.

Figure 7 and Figure 8 show the output sets for the healthy and faulty models after the auxiliary input signal designed with the method proposed is injected into the system from $k = 20$ until $k = 23$ and from $k = 40$ until $k = 43$, respectively. In these figures, the red zonotopes are the output sets of the healthy model, and the blue zonotope are the output sets of faulty model, respectively. Black circles represent the output of the actual system. In Figure 7, the actual system output falls in the output zonotope of the faulty model at $k = 21$. This means that the fault is detected since $k = 21$, because at $k = 20$ the actual output was still in output zonotope of the healthy model. According to (59), the system present the fault from $k = 20$, so there is time

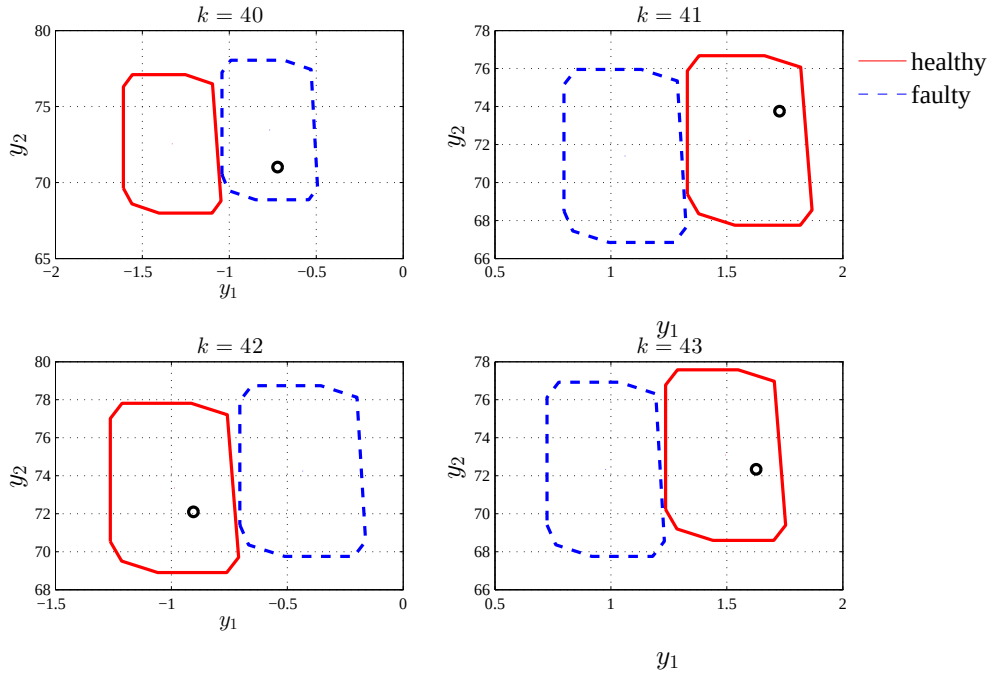


**FIGURE 8** The output sets of healthy and faulty model obtained by the proposed method.

delay of one sample time in the fault detection process. Similarly, the output of actual system falls in the output zonotope of the healthy model at $k = 41$, so the system is detected to be in the faulty state at this time.

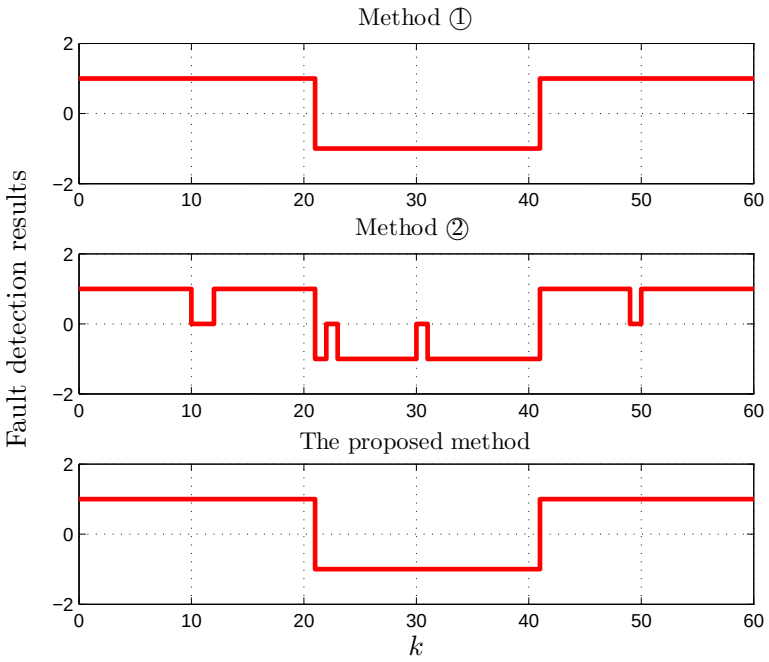


**FIGURE 9** The result of fault detection.

The comparison of the fault detection results between the proposed method and methods ① and ② are presented in Figure 9. These result are obtained by checking the conditions (53) with the method proposed in Remark 2. Since method ② does not consider the system parameter uncertainties, it may generate some wrong fault detection results.

According to Figure 4 and Figure 9, the auxiliary input signal obtained by the method ② is the smallest, but the detectability of faults is poor. Method ① presents satisfactory detection results, but the auxiliary input signal is big (see Figure 4). Compared to the other two methods, the proposed method has a small auxiliary input signal and can correctly detect the system model. In summary, the proposed method has advantages because of the smaller auxiliary input signals required while presenting satisfactory detection results.

## 6 | CONCLUSIONS

In this paper, an active FD method based on set-membership approach for uncertain discrete-time system is proposed. Firstly, a zonotopic observer is designed with the aim of minimizing the set that bounds the output estimated set. This is achieved by means of a time-varying gain of the observer that is obtained by minimizing the size of the zonotope bounding output sets. Then, a proper auxiliary input signal is designed to separate the output zonotopes of the healthy model from the output zonotopes of the faulty model. Finally, the input signal is injected into the system to detect small faults. Based on the results obtained using the considered case study, the proposed method reduces the size of the output zonotopes and conservativeness of the auxiliary input signal design process by using zonotpic observers. Since the auxiliary input signal belongs to an external signal, the addition of the auxiliary input signal will have an impact on the system. Therefore, a method for further reducing the conservativeness will be focused on in future research.

## ACKNOWLEDGMENTS

J. Wang is thankful for the grant funded by NSFC (61973023, 61573050) and the Fundamental Research Funds for the Central Universities (No. XK1802-4).
M. Zhou is thankful for the grant funded by NSFC (51805021) and China Postdoctoral Science Foundation Grant (No. 2018M631311).

## References

1. Xu F, Tan J, Wang X, et al. Generalized set-theoretic unknown input observer for LPV systems with application to state estimation and robust fault detection. *Int J Robust Nonlinear Control.* 2017; 27: 3812 – 3832.
2. Wang Y, Puig V, Cembrano G. Robust fault estimation based on zonotopic Kalman filter for discrete-time descriptor systems. *Int J Robust Nonlinear Control.* 2018; 28(16): 5071 – 5086.
3. Li X, Zhu F. Fault-tolerant control for Markovian jump systems with general uncertain transition rates against simultaneous actuator and sensor faults. *Int J Robust Nonlinear Control.* 2017; 27(18): 4245 – 4274.
4. Nikoukhah R, Campbell S, Drake K. An active approach for detection of incipient faults. *Int J Syst Sci.* 2010; 41: 241 – 257.
5. Pourasghar M, Puig V, Ocampo-Martinez C. Interval observer versus set-membership approaches for fault detection in uncertain systems using zonotopes. *Int J Robust Nonlinear Control.* 2019; 29: 2819 – 2843.
6. Zhou M, Wang Z, Shen Y, Shen M. H_/H∞ fault detection observer design in finite-frequency domain for Lipschitz nonlinear systems. *IET Control Theory Appl.* 2017; 11(14): 2361 – 2369.
7. Zhang Q, Geng S. Dynamic uncertain causality graph applied to dynamic fault diagnoses of large and complex systems. *IEEE Trans Reliability.* 2015; 64(3): 910 – 927.
8. Kallas M, Mourot G, Maquin D, Ragot J. Data-driven approach for fault detection and isolation in nonlinear system. *Int J Robust Nonlinear Control.* 2018; 32: 1569 – 1590.

9. Cai B, Zhao Y, Liu H, Xie M. A data-driven fault diagnosis methodology in three-phase inverters for PMSM drive systems. *IEEE Trans Power Electronics.* 2017; 32(7): 5590 – 5600.

10. Šimandl M J, Punčochář I. Active fault detection and control: Unified formulation and optimal design. *Automatica.* 2009; 45: 2052 – 2059.

11. Punčochář I, Škach J. A survey of active fault diagnosis methods. *IFAC-PapersOnline.* 2018; 51(24): 1091 – 1098.

12. Wang J, Zhang J, Qu B, Wu H, Zhou J. Unified architecture of active fault detection and partial active fault-tolerant control for incipient faults. *IEEE Trans Syst Man Cybernetics Syst.* 2017; 47(7): 1688 – 1700.

13. Marseglia G, Raimondo D. Active fault diagnosis: A multi-parametric approach. *Automatica.* 2017; 79: 223 – 230.

14. Kerestecioğlu F, Çetin I. Optimal input design for the detection of changes towards unknown hypotheses. *Int J Syst Sci.* 2004; 35(7): 435 – 444.

15. Škach J, Punčochář I, Lewis F. Optimal active fault diagnosis by temporal-difference learning. In: Proceedings of IEEE 55th Conference on Decision and Control. ; December 12 – 14, 2016; Las Vegas, USA.

16. Garulli A, Vicino A. Set membership localization of mobile robots via angle measurements. *IEEE Trans Robot Autom.* 2001; 17(4): 450 – 463.

17. Puig V, Pourasghar M. Fault Diagnosis Using Set-Membership Approaches. *Fault Diagnosis of Dynamic Systems* 2019: 237–261.

18. Zhai S, Wang W, Ye H. Auxiliary signal design for active fault detection based on set-membership. *IFAC-PapersOnLine.* 2015; 48(21): 452 – 457.

19. Wang J, Wang J, Zhou J. On-line active fault detection based on set-membership ellipsoid and moving window. In: Proceedings of IEEE 7th Data Driven Control and Learning Systems Conference. ; 2018: 420 – 425.

20. Scott J, Findeisen R, Braatz R, Raimondo D. Design of active inputs for set-based fault diagnosis. In: Proceedings of American Control Conference. ; 2013; Washington, DC, USA.

21. Raimondo D, Marseglia G, Braatz D, Scott J. Closed-loop input design for guaranteed fault diagnosis using set-valued observers. *Automatica.* 2016; 74: 107 – 117.

22. Tabatabaeipour S. Active fault detection and isolation of linear time varying systems: a set-membership approach. *Int J Syst Sci.* 2013: 1917 – 1933.

23. Campbell S, Horton K, Nikoukhah R. Auxiliary signal design for rapid multi-model identification using optimization. *Automatica.* 2002; 38: 1313 – 1325.

24. Campbell S, R N. *Auxiliary signal design for failure detection*. Princeton University Press . 2004.

25. Zhou M, Cao Z, Zhou M, Wang J, Wang Z. Zonotoptic fault estimation for discrete-time LPV systems with bounded parametric uncertainty. *IEEE Trans Intell Transp Syst.* 2019. doi: 10.1109/TITS.2019.2898853.

26. Combastel C. Merging Kalman filtering and zonotopic state bounding for robust fault detection under noisy environment. *IFAC – PapersOnLine.* 2015; 48(21): 289 – 295.

27. Alamo T, Bravo J, Camacho E. Guaranteed state estimation by zonotopes. *Automatica.* 2005; 41(6): 1035 – 1043.

28. Le V, Stoica C, Alamo T, Camacho E, Dumur D. Zonotopic guaranteed state estimation for uncertain systems. *Automatica.* 2013; 49: 3418 – 3424.

29. Wang Y, Puig V, Cembrano G. Set-membership approach and Kalman observer based on zonotopes for discrete-time descriptor systems. *Automatica.* 2018; 93: 435 – 443.

30. Combastel C. A state bounding observer for uncertain non-linear continuous-time systems based on zonotopes. In: Proceedings of the 44th IEEE Conference on Decision and Control. ; December 12 – 15, 2005; Seville, Spain: 7228 – 7234.

31. Scott J, Findeisen R, Braatz R, Raimondo D. Input design for guaranteed fault diagnosis using zonotopes. *Automatica.* 2014; 50(6): 1580 – 1589.

32. Dobkin D, Hershberger J, Kirkpatrick D, Suri S. Computing the intersection-depth of polyhedra. *Algorithmica.* 1998; 9: 518 – 533.

33. Pourasghar M, Puig V, Ocampo-Martinez C. Characterisation of interval-observer fault detection and isolation properties using the set-invariance approach. *Journal of the Franklin Institute.* 2019.

34. Wang Y, Wang Z, Puig V, Cembrano G. Zonotopic set-membership state estimation for discrete-Time descriptor LPV systems. *IEEE Trans Autom Control.* 2019; 64(5): 2092 – 2099.

35. Combastel C. Zonotopes and Kalman observers: Gain optimality under distinct uncertainty paradigms and robust convergence. *Automatica.* 2015; 55: 265 – 273.

36. Bertsekas D. *Nonlinear programming*. Belmont, MA: Athena Scientific . 1999.

37. Zhang J, Yuan C, Stegagno P, zang W, Wang C. Small fault detection from discrete-time closed-loop control using fault dynamics residuals. *Neurocomputing.* 2019; 365: 239 – 248.